Deformation and sedimentary responses to top-to-north shear along the range front of the Big Band of the Ailao Shan–Red River shear zone and its origin, SE edge of the Tibetan Plateau

Erchie Wang[1], Chun Fan[2], and Zhe Su[3]

[1]Institute of Geology and Geophysics, CAS
[2]School of Energy Resources, China University of Geosciences
[3]National Institute of Natural Hazards, Ministry of Emergency Management of China

November 22, 2022

Abstract

Understanding the mountain–basin coupling relationship is fundamental to placing constraints on the tectonic evolution of the Ailao Shan–Red River mylonite shear zone, the key feature accommodating relative movement between the Tibetan Plateau and SE Asia, because a contemporary basin bounds its middle segment on the northeast, along which the shear zone is bent from northwest–southeast to roughly east–west. The basin comprises two units: the Mubang Breccia and the Lengdun Conglomerate of Early Oligocene and Late Oligocene–Early Miocene age, respectively. This study reveals evidence indicating that the Wubang Breccia marks a high-strain zone, resulting from top-to-north shear (range-front detachment (RFD)), along which the mylonite on the footwall experienced northward bending. Moreover, the Lengdun Conglomerate on the hanging wall was deposited as growth strata, overlying a thrust belt to the north. The latter marks the southern rim of the Yangtze block, composed of landslide blocks, whose northward displacement along the toe of the RFD was synchronized with the north–south extension across the Red River basin. The spatial and temporal relationships between the Red River basin and the Ailao Shan–Red River shear zone indicate that basin formation was controlled by the change in geometry of the shear zone. The Red River basin can be viewed as an extensional step-over in the left-lateral strike-slip field, in which all sedimentary and deformation processes are the manifestation of the gravitational collapse, accommodated by the RFD. This indicates that the sedimentary detritus, including both landslide blocks and the Langdun Conglomerate, were all shed from the top of the Ailao Shan mylonite belt. The cause of bending of the shear zone is attributed to the northward movement between India and South China.

Deformation and sedimentary responses to top-to-north shear along the range front of the Big Band of the Ailao Shan–Red River shear zone and its origin, SE edge of the Tibetan Plateau

Erchie Wang[1] Chun Fan[2] Zhe Su[3]

1. Institute of Geology and Geophysics, CAS, 100029, China

2. School of Energy Resources, China University of Geosciences, Beijing, 100083, China,

3. National Institute of Natural Hazards, Ministry of Emergency Management of China, Beijing, China

Abstract

Understanding the mountain–basin coupling relationship is fundamental to placing constraints on the tectonic evolution of the Ailao Shan–Red River mylonite shear zone, the key feature accommodating relative movement between the Tibetan Plateau and SE Asia, because a contemporary basin bounds its middle segment on the northeast, along which the shear zone is bent from northwest–southeast to roughly east–west. The basin comprises two units: the Mubang Breccia and the Lengdun Conglomerate of Early Oligocene and Late Oligocene–Early Miocene age, respectively. This study reveals evidence indicating that the Wubang Breccia marks a high-strain zone, resulting from top-to-north shear (range-front detachment (RFD)), along which the mylonite on the footwall experienced northward bending. Moreover, the Lengdun Conglomerate on the hanging wall was deposited as growth strata, overlying a thrust belt to the north. The latter marks the

southern rim of the Yangtze block, composed of landslide blocks, whose northward displacement along the toe of the RFD was synchronized with the north–south extension across the Red River basin. The spatial and temporal relationships between the Red River basin and the Ailao Shan–Red River shear zone indicate that basin formation was controlled by the change in geometry of the shear zone. The Red River basin can be viewed as an extensional step-over in the left-lateral strike-slip field, in which all sedimentary and deformation processes are the manifestation of the gravitational collapse, accommodated by the RFD. This indicates that the sedimentary detritus, including both landslide blocks and the Langdun Conglomerate, were all shed from the top of the Ailao Shan mylonite belt. The cause of bending of the shear zone is attributed to the northward movement between India and South China.

Keywords: Tibetan Plateau, Ailao Shan–Red River shear zone, stretch lineation, detachment fault, denudation, growth strata, landslides, clockwise bending

INTRODUCTION

The growth of the Tibetan Plateau is largely accommodated by strike-slip faults. One of the largest is the Ailao Shan–Red River shear zone (ARSZ), a more than 1800-km-long crustal discontinuity that can be traced from the southeastern edge of the Tibetan Plateau southeastward to the South China Sea (Fig. 1).
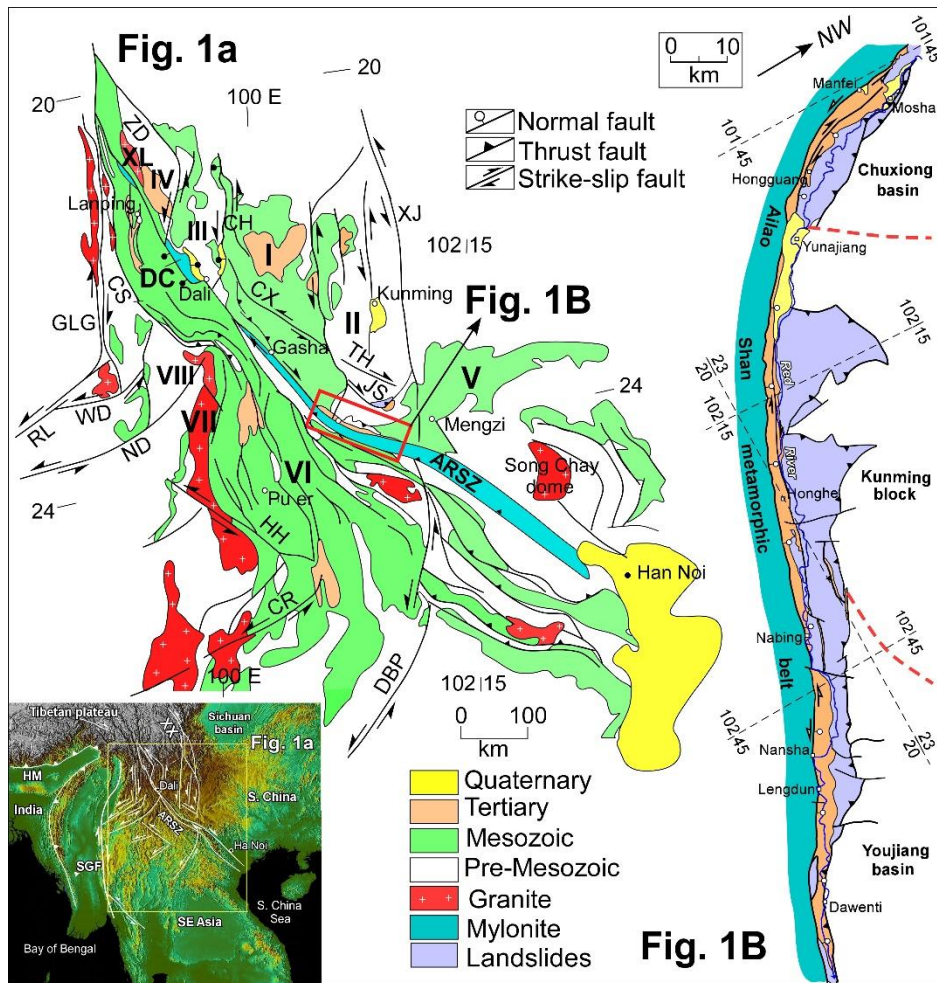
Figure 1. (**A**) Major tectonic elements within the Yangtze platform and Three River fold belt bounding the ARSZ on the northeast and southwest. (**B**) Simplified geological map of the NE foreland of the Big Band of the ARSZ, including Red River basin fills and the southern rim of the Yangtze platform; the latter exhibits strong deformation, assigned as landslide blocks. I: Chuxiong basin; II: Kunming block; III: Dali block; IV: Shigu block; V: Youjiang fold belt; VI: Lanping–Simao basin; VII: Lincang batholiths; VIII: Baoshan block; VIIII: Tengchong block; CX: Chuxiong fault; NT: Nandinghe fault; HE: Heihe fault; SG: Saging fault; JS: Jianshui fault; ARSZ: Ailao Shan–Red River shear zone; DC: Diancang Shan massif; XL: Xuelong Shan massif; TH: Tonghai fault; JS: Jiangshui fault; HQ: Heqing fault; CH: Chenghai fault; ZD: Zhongdian fault; CS: Congshan shear zone; XX: Xianshuihe–Xiaojing fault.

The outstanding features of the ARSZ make it distinct from other strike-slip faults within the Tibetan Plateau. These include the following: **(1)** It is the only fault to have had its shear sense reversed through time, beginning with left-lateral movement along the Ailao Shan metamorphic belt that accommodated the southeastward extrusion and

rotation of SE Asia with respect to South China from 25 to 19 Ma (Tapponnier et al.,

1986; Harrison et al., 1992, 1996; Leloup et al., 1993, 2001; Schärer et al., 1990, 1994)

and changing to right-lateral movement along the Red River fault in the Late Cenozoic at

4.7 Ma as a result of the eastward extrusion of South China with respect to SE Asia

(Leloup et al., 1993; Harrison et al., 1996). Other geochronological data suggest that its

strike-slip motion started during 35–32 Ma (Schärer et al., 1990). Searle (2010)

demonstrated that the ARSZ present with lower temperature fabrics and argued that its

left-lateral shear started much earlier (21 Ma) than previously thought. **(2)** It is the only

faults with its strike-slip movement resulting in the uplift and exhumation of the deep

crust, forming the Ailao Shan mylonitic belt, but the uplift mechanism remains

controversial. At least two processes have been suggested. The earlier one was

synchronized with the left-lateral motion (Tapponnier et al., 1990; Harrison et al., 1992,

1996; Leloup et al., 1993, 1995, 2001; Schärer et al., 1990, 1994; Jolivet et al., 2001)

and the later one was associated with post-Miocene right-lateral motion with a vertical

slip component (Allen et al., 1984; Replumaz et al., 2001; Schoenbolhm et al., 2006), the

latter causing a large part of the uplift, as shown by the east-dipping escarpments

present along the NE edge of the shear zone (Tapponnier et al., 1990). However, there

is no sign indicating active movement along the Red River fault (Searle, 2006). In

addition, in many places, the foliation cropping out along the NE edge of the middle

segment of the metamorphic belt dip inwardly to the southwest, which is thus considered

to mark a thrust fault. This brought the metamorphic belt to the surface, being

associated with the foreland filled with the Lengdun Formation (Bureau of Geology and

Mineral Resources of Yunnan Province, 1991; Schoenbolhm et al., 2005; Wang et al., 2016). Moreover, according to Wang and Burchfiel (1997) and Burchfiel et al. (2008), the ARSZ formed as a transpressional transfer fault, lying above a midcrustal detachment, with its left-lateral movement largely absorbed by shortening across the adjacent Lanping–Simao basin to the southwest, leading to the uplift of the metamorphic belt. **(3)** The shear zone is highlighted by a linear basin built along the NE foot of the middle segment of the shear zone (referred to here as the Red River basin). This zone is filled with two sedimentary units, the Wubang Breccia of Oligocene age and the Lengdun Conglomerate of Late Oligocene–Early Miocene age. Although it is widely accepted that determining the mountain–basin coupling relationship is the key to reveal the orogenic process, thus far, studies on the Red River basin and Ailao Shan mylonite belt have been conducted separately. The NW-trending ARSZ is apparently bent to the east–west direction along its middle segment (referred to as the Big Band). This is generally believed to have been caused by the southward movement along the Xiansuihe–Xiaojiang fault, known as one of the most active strike-slip faults within the Tibetan plateau owing to its left-lateral movement (Wang et al., 1998; Schoenbohm et al., 2006). Nevertheless, we noted that the Big Band is being bounded by the Red River basin on the north, implying that the basin formation must be correlated with the change in geometric shape of the shear zone. Our five-year field study focused on the deformation and sedimentation within the Red River basin and its wall rocks, including the Ailao Shan mylonite belt on the south and the sedimentary cover rocks of the Yangtze block on the south. Many new rock outcrops have been exposed by road construction in the past 10

years. These allow us closely to observe the Red River basin and its wall rocks. The new results reveal that the range-front deformation and sedimentation were not directly controlled by the left-lateral movement but by the N–S extension. This was accommodated by a north-dipping detachment, referred to as range-front detachment (RFD). Based on these new findings, the tectonic evolution of the ARSZ is revisited.

GEOLOGICAL SETTING

The main part of the generalized ARSZ extends along the boundary between the Yangtze block to the northeast and the Three River fold belt to the southwest (Fig. 1**)**. The Yangtze platform has behaved as a stable platform, comprising three major tectonic elements: the Chuxiong basin on the west, the Kunming block in the middle, and the Youjiang fold belt on the east. The Chuxiong basin consists of a crystalline basement of Early Proterozoic age and a terrestrial sedimentary cover that exhibits a continuous succession with age ranging from the Triassic to the Eocene. The Kunming block is composed of a crystalline basement of Early Proterozoic age and sedimentary cover rocks. The latter is divided into two parts: The lower part is characterized as oceanic facies with age ranging from the Sinian to the Middle Triassic, and the upper part is characterized by terrestrial facies with age ranging from the Late Triassic to the Eocene. The Youjiang fold bet consists mostly of marine strata of Triassic age, with the lower and upper parts dominated by carbonate and flysch succession. The Yangtze platform is ruptured in a N–S direction by the Xianshihe–Xiaojiang fault, one of the most active features within the Tibetan Plateau, as a result of its left-lateral movement, dated as the Late Miocene (~12 Ma). It dies out southward within a series of extensional basins of Pliocene–Quaternary

age to the north of the ARSZ (Wang et al., 1998).

The Three River fold belt is described as a tectonic collage with prolonged history, along which the Mekong, Salween, and Jinsha rivers flow to the south, which endow the fold belt with its name. The belt consists of four major tectonic elements: From east to west, these are the Lanping–Simao basin, the Lincang batholiths, the Baoshan block, and the Tentchong block (Wang and Burchfiel, 1997).

The ARSZ crops out along a belt of metamorphic rocks that have a long evolutionary history (Leloup et al., 1995; Searle et al., 2010; Liu et al., 2012), having experienced intensive mylonitization as a result of left-lateral shear, taking place at a depth of 15–20 km, during the Late Oligocene to the Miocene (35–17 Ma) (Tapponnier et al., 1986, 1990; Harrison et al., 1992, 1996; Leloup et al., 1993, 1995, 2001; Schärer et al., 1990, 1994). Other geochronological data suggest that its strike-slip motion started after 35–32 Ma (Schärer et al., 1990; Jolivet et al., 2001). Searle (2006) demonstrated that the ARSZ presents with lower temperature fabrics and argued that its left-lateral shear post-dated metamorphism and started much earlier (21 Ma) than previously thought (35 Ma). The southwest boundary of the ARSZ is considered to be thrust fault, dividing the high-grade metamorphic rocks to the hanging wall and the Mesozoic succession of the Lanping–Simao basin and its basement of Paleozoic age to the footwall, but at present there is no sign of activity (Tapponnier et al., 1990; Leloup et al., 1995) **(**Fig. 1**)**.

The Red River flows to the southeast along the northeast foreland of the ARSZ (Fig. 2). Clark et al. (2004) presented a reconstructed river network in which the upper reaches of the Salween, Mekong, and Yangtze rivers drained through the Red River as an axis river

into the South China Sea prior to the Miocene. However, the coeval sediments are only preserved along a linear intermountain basin, distributed on the NE piedmont of the Big Band, called the Red River basin. The fills comprise two sets of strata, the Wubang Mudstone and the Lengdun Formation, which can be assigned as Early Oligocene and Late Oligocene–Miocene in age, respectively (Schoenbohm et al., 2005). All the strata experienced varying degrees of deformation, resulting from either left-lateral or right-lateral movement of the shear zone (Allen et al., 1984; Clark et al., 2004; Schoenbohm et al., 2005). A special study of the Wubang Mudstone and Lengdun Formation was given by Schoenbohm et al. (2005). There are some isolated outcrops making up of bolder conglomerate, assigned as Early Pleistocene in age, occurring along either the shoulder or the bottom of the Red River valley as terrace deposits (Fig. 1). In the following we describe the sedimentary and deformation features of the Red River basin and its wall rocks, including the mylonite rocks and the Yangtze block enclosing the basin on the south and north. Our results reveal the following: 1. The Wubang Mudstone is highly brecciated, being characterized as a strong strain zone (the Wubang Breccia). 2. The mylonite bounding the Red River basin on the south experienced unique tractional deformation. 3. The Lengdun Formation presents with the unique feature of growth strata (the Lengdun Conglomerate). 4. The Yangtze block bounding the basin on the north is deformed as a north-directed thrust-fold belt, made up of landslide blocks. All these features are interpreted to reflect the top-to-north shear along a north-dipping normal fault (RFD). The following are described in order.
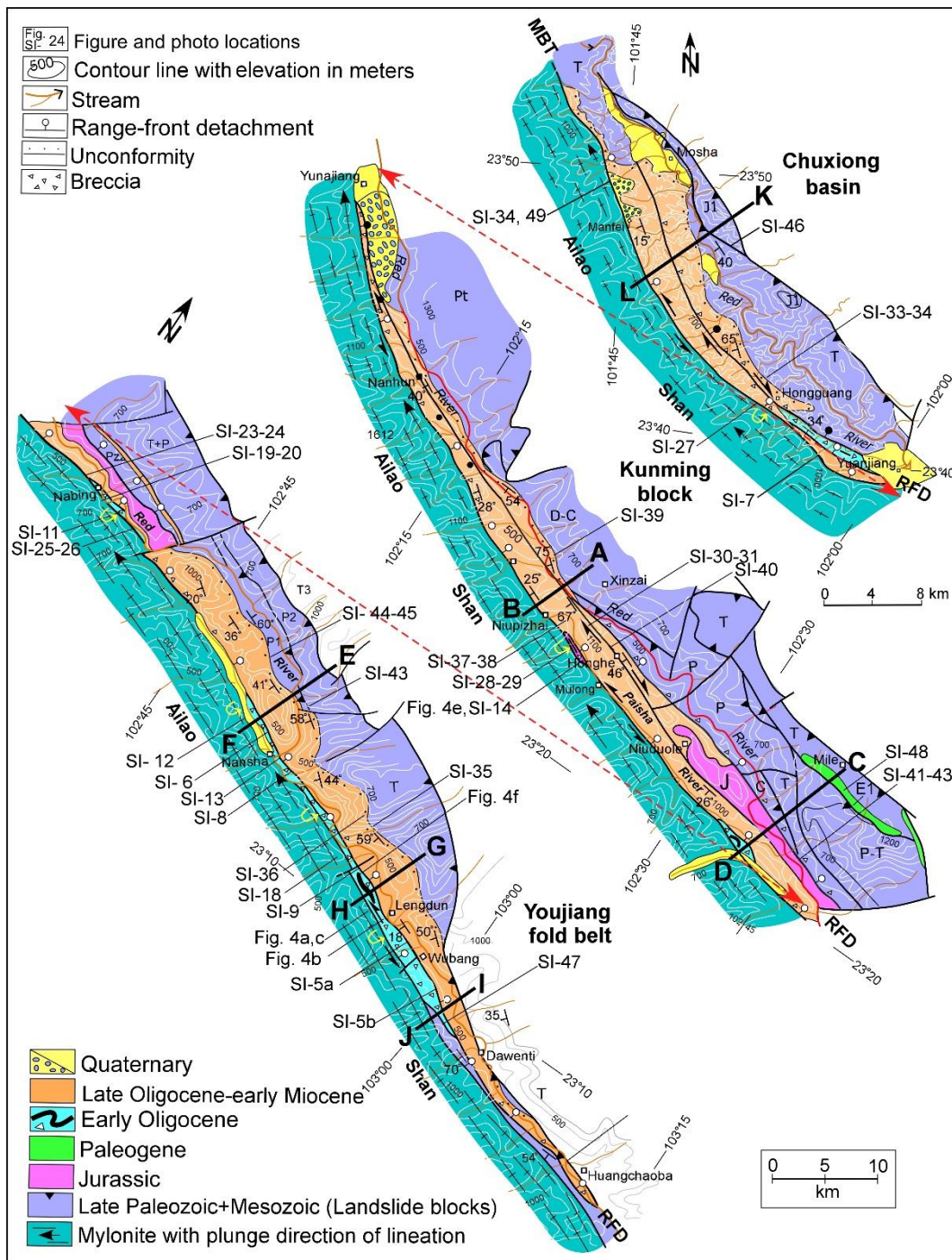
Figure 2. Geologic and topographic map of the Red River basin and its marginal areas covering the Yangtze platform, with its southern rim defined as landslide blocks, and the Ailao Shan metamorphic belt. MBT: main boundary fault; RFDF: RFD fault.

9
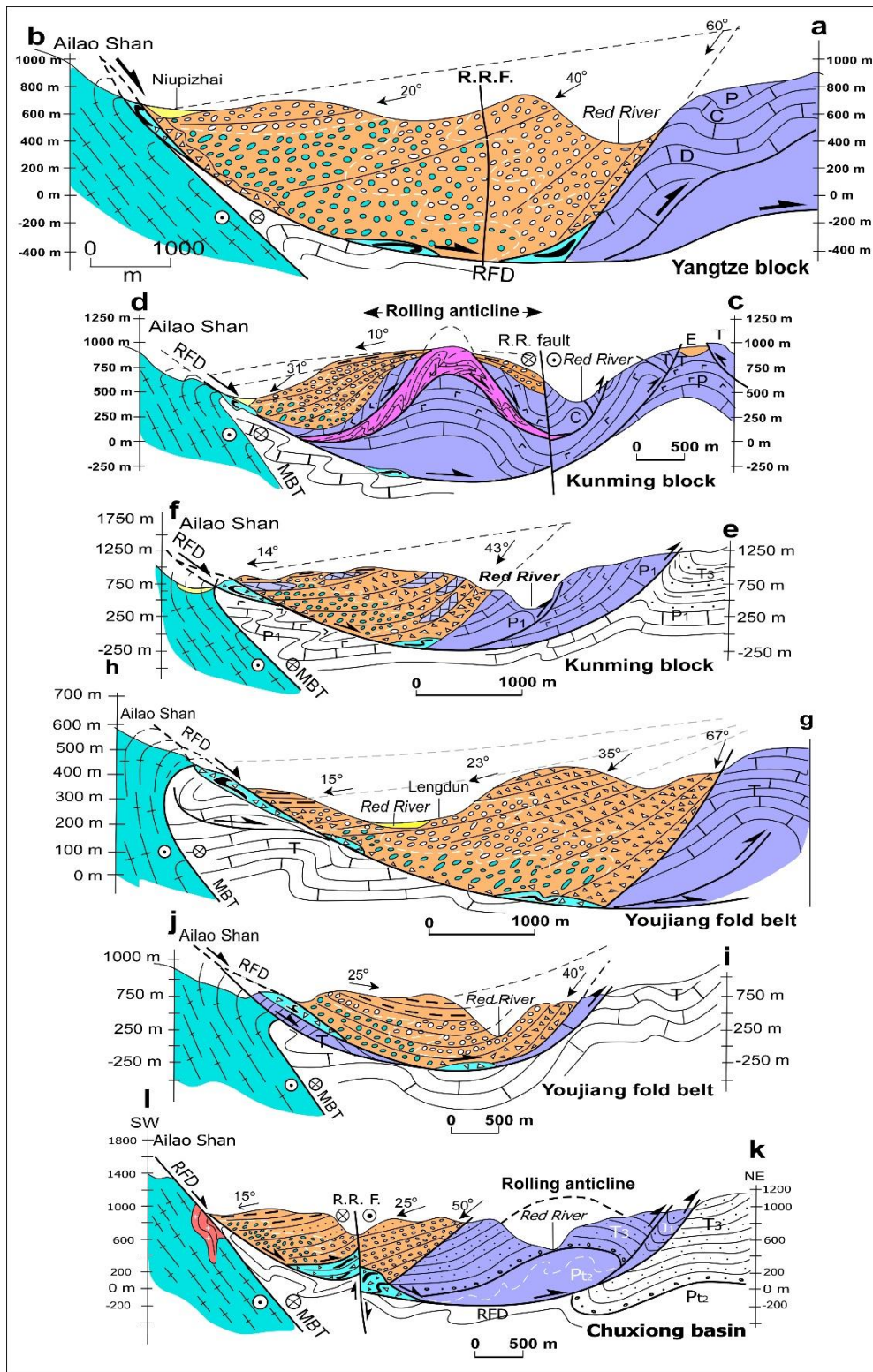
Figure 3. Cross sections of the Red River basin and its wall rocks, the mylonitic belt on the south, and the Yangtze block on the north. The southern edge of the Yangtze block is rimmed by a thrust-fold belt, interpreted as consisting of landslide blocks. The range-front deformation and sedimentary feature are interpreted as reflecting the top-to-north shear along a north-dipping detachment fault (RFD) in the areas of Honghe (a and b), Niuduole (c and d), Nansha (e and f), Lengdun (g and h), Wubang (i and j), and Mosha (k and l).

DEFORMATION OF THE WUBANG BRECCIA RESULTING FROM TOP-TO-NORTH SHEAR

The Wubang Mudstone discontinuously extends along the foothills of the Big Band of the mylonitc belt as a series of lens-shaped belts in the area between the Yuanjiang and Dawenti, dividing the Lengdun Conglomerate to the north and the metamorphic belt to the south (Figs. 2, 3, 4b, d and e). Where it pinches out, the Lengdun Conglomerate directly overlays the metamorphic rocks (SI-11).
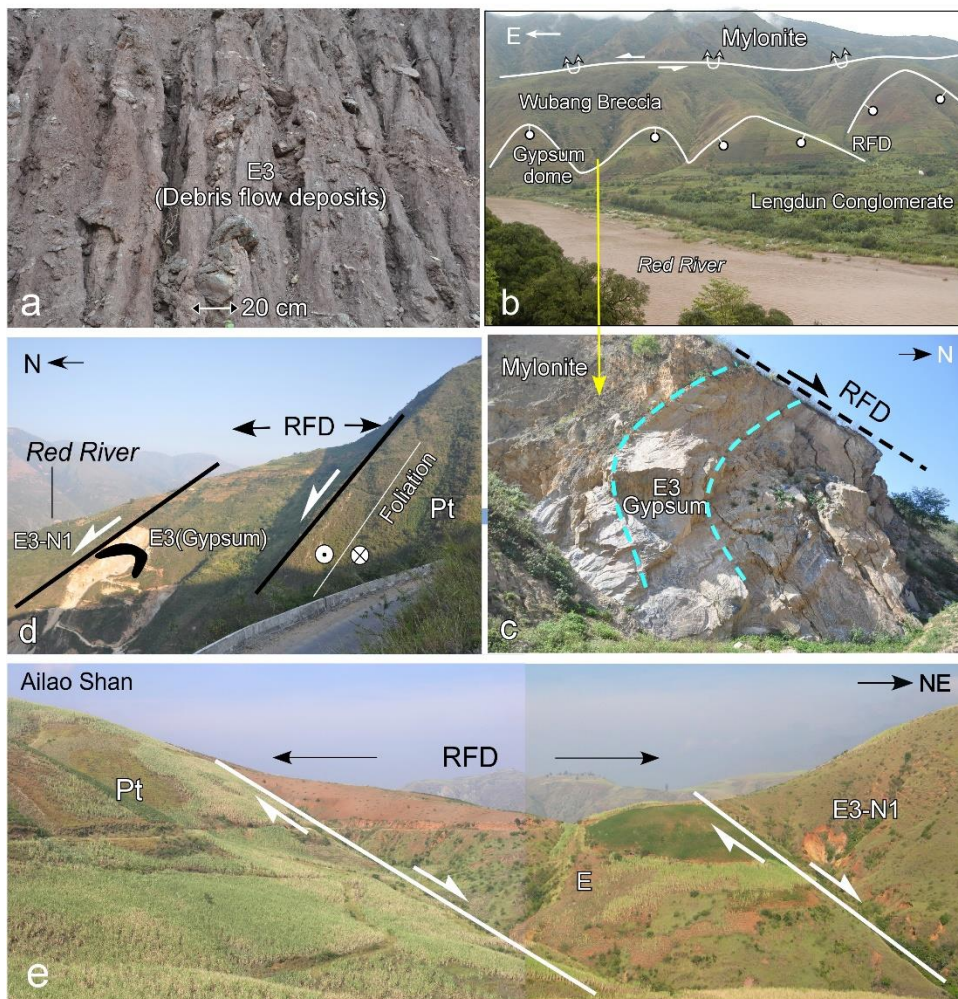
Figure 4. Photographs of the Wubang Breccia, showing its sedimentary and deformation features and its relationship with the mylonitic belt and the Lengdun Conglomerate. **(a)** View south at the northern foothills of the Ailao Shan, with the RFD shown by the Wubang Breccia and its boundary faults, marked by the triangular fault scarps, 3000 m south of Lengdun. **(b)** Close-up view of the Wubang Breccia; it is characterized by poorly sorted debris flow deposits, consisting of sandstone breccia, supported by fine-grained mudstone as its matrix, 2000 m south of Lengdun. **(c)** View west at the gypsum layer within the Wubang Breccia in **b**, bending to the north, dragged by the top-to-north shear along the RFD. **(d)** View east at the RFD dipping to the north, defined by the Wubang Breccia, dividing the Lengdun Conglomerate to the hanging wall and the mylonite to the footwall, 3000 m south of Lengdun. **(e)** View west at the RFD, dipping to the north at low angle, defined by the Wubang Breccia, dividing the Lengdun Conglomerate to the north and the mylonite to the south, 3000 m southwest of Honghe. **(f)** View north at the Wubang Breccia, characterized as a poorly sorted debris flow deposit, which is offset by a N-dipping detachment, probably associated with the RFD.

The protolith of the Wubang Breccia is characterized by purple-colored, fine-grained lacustrine deposits, bearing with evaporate, as described by Schoenbohm et al. (2005). However, based on our field observations, these deposits have been entirely brecciated and their original sedimentary texture has been totally destroyed. For this reason, we refer it them as the Wubang Breccia, exhibiting the following evidence as a high strain zone, resulting from top-to-north shear, referred to herein as the RFD. The Wubang Breccia is characterized as debris flow deposits, with rigid sandstone broken into breccia, which are formed as detritus (Figs. 4b, 4f and SI-9). They are supported by a matrix defined by intensively sheared mudstone, and some of the breccia were reworked to form massive to crudely stratified debris-flow deposits with outsized angular boulders. The contained gypsum and marl were plastically extruded into the country rocks to form a series of domes and veins (Figs. 4c and SI-10). It is crucial to note that, in many places, these debris flow deposits are penetrated by many small normal faults, mostly dipping to the north at low angle (SI-9). However, these faults are very short and discontinuous, vanishing within the debris flow deposits. This implies that debris flow deposition took place while the basin

underwent extension.

The northern boundary of the Wubang Breccia is considered to be either an unconformity (Bureau of Geology and Mineral Resources of Yunnan Province, 1991) or a fault contact, defined as the Red River fault (Schoenbohm et al., 2005). Based on our field observations, this boundary dips to the north at various dipping angles. Both the Lengdun Conglomerate and the Wubang Breccia are sheared along this boundary into poorly sorted breccia and fault gouge (Fig. 4f, SI-5-9; see Fig. 2 for locations), but there is no sign indicating that it is still active (SI-6). In the areas of Nansha, Lengdun, and Honghe (Figs. 2 and 3), both gypsum and marl layers within the Wubang Breccia are strongly deformed in a plastic pattern, manifested as rootless folds, with the axis overturned to the north, exhibiting top-to-north shear (Fig. 4c, SI-10, SI-13, and SI-14).

All these deformation patterns indicate that the Wubang Breccia marks a high-strain zone, with the folded gypsum and marl layers formed as strain markers, exhibiting the top-to-north shear (Figs. 2 and 3). We tentatively regard this breccias zone as a normal fault dipping to the north (RFD), accommodating divergent movement between the mylonite belt and its adjacent foreland (Fig. 5). Observably, both the gypsum and marl serve as ideal lubricants for the detachment shear.

DEFORMATION OF THE MYLONITE RESULTING FROM TOP-TO-NORTH SHEAR

The architecture of the Ailao Shan mylonitic belt is clearly defined by foliation and lineation. From Mosha to the northwest, along the base of the escarpments shaping the NE boundary of the Ailao Shan mylonitic shear zone, foliations are exposed at the surface dipping to the NE along the northwestern section at high angles (60°–70°). The stretching

lineations are widely developed on the foliations, being defined by elongated mineral aggregates (Tapponnier et al., 1990; Harrison et al., 1996). Their eastern edge is highlighted by a series of triangular fault facets sloping up to 60° NE with 200–500 m of topographic relief, referred to as the Main Boundary fault (MBT), juxtaposing the mylonitic rocks with the clastic rocks of Triassic age of the Chuxiong basin (Figs. 1 and SI-15, see Fig. 5 for location). These fault scarps are generally considered to mark the trace of normal faults, having formed either in the post-Miocene time (Tapponnier et al., 1990) or in the Early Miocene (Harrison et al., 1992; Schärer et al., 1994). However, there is no sign indicating any active movement along the Red River fault (Searle, 2006, 2010), and there is a lack of post-Miocene sediments within the foreland of the metamorphic belt. Moreover, based on our field observations, these foliations are penetrated by subhorizontal stretching lineation exhibiting left-lateral shear.


14
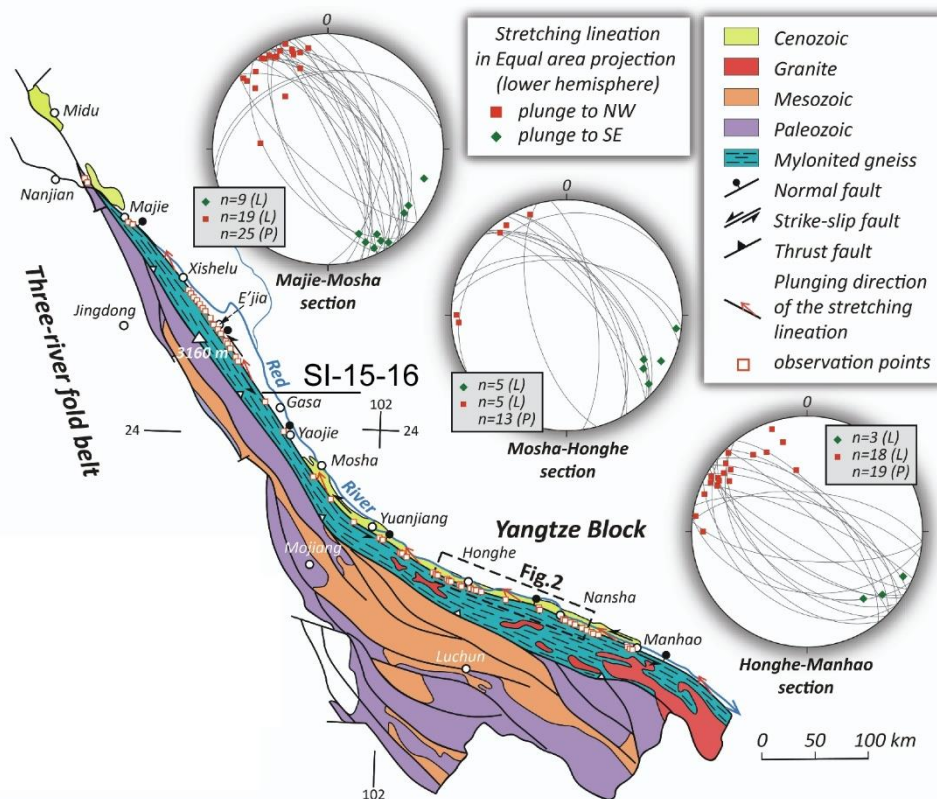
Figure 5. Generalized geologic map of the ARSZ, bounded on the southwest by a Paleozoic lower grade metamorphic belt and on the northeast by Tertiary strata. Lower hemisphere stereonet projections of 59 stretch lineations cropping out along the NE edge of the Ailao Shan metamorphic belt.

In this field study, we systemically measured the plunge direction and angle of the stretching lineation along the NE base of the entire Ailao Shan mylonite belt in China, from Majie southward to Manhao (Fig. 4 and Table 1). The stretching lineation are defined by elongate mineral aggregates such as quartz rods and orientated feldspar and mica. Importantly, there is no the residual stretching lineation with slightly different plunging angles at the same location observed, indicating that the fault is always moving in the same direction. Because the ductile shear always occurs at lower temperature (Searle, 2006), the possibility that the older stretching lineations have been totally erased by the last phase of the left-slip shear is unlikely.

Our results from 59 measurements are shown in Fig. 4. They reveal very regular attitudes for the stretching lineation, 42 of which plunge to the northwest, with an average plunge value of 12.76° (Table 1). We note that 23 of the 42 plunging angles are <10°, with an average value of 6.43°. There are 17 lineations plunging to the southeast. In addition, the mylonites within the core of the Ailao Shan metamorphic belt also display stretching lineation, plunging to the northwest at a low angle (Tapponnier et al., 1990). This implies that the left-lateral movement along the Ailao Shan mylonitic belt had a minor component of vertical movement, by which the metamorphic rocks got uplifted, probably being drowned out from the deep crust underneath the Midu Gap to the northwest, as proposed by Leloup et al. (1995). The eastern boundary of these foliations (MBT in Figs. 2 and 3) were cut into a series of triangular fault facets by the river incision

and present a false image of the normal fault facets (Fig. 4 and SI-16-17, see Fig. 5 for location).

However, from Mosha to the southeast, the northern margin of the Big Band of the ARSZ displays much gentler topography along its NE edge (SI-18; see Fig. 2 for location), and the mylonite cropping out along its NE edge vary in dipping direction, with some dipping to the northeast while others dipping inwardly to the southwest. For this reason, some researchers have concluded that the foliation dipping inwardly to the south represents a thrust fault, which brought the mylonite to the surface, associated with the deposition of the Lengdun Formation (Bureau of Geology and Mineral Resources of Yunnan Province, 1991; Schoenbohm et al., 2006).

With newly exposed outcrops along the road cuts in the Nabing and Daheigong areas between Honghe and Nansha, we observed a series of recumbent folds in the mylonite, where the foliation gently dips downward to the southwest (200°), then gradually steepens to fold back to the northeast at a high angle (SI-21–24; see Fig. 2 for locations). In the areas south of Lengdun and Wuang, the main boundary fault of the Ailao Shan belt (MBT) is also seen to be bended to the north, overlapping the Wuang Mudstone (Fig. 4a and c and SI-10). In the area northwest of Yuanjiang basin, 3 km west of Hongguang, a porphyry intrusion, ~200 m long, with an age estimated as 20–40 Ma, intruded into the boundary between the mylonitic belt and the Lengdun Formation, which is also bent to the north (SI-27). Our field mapping and observations revealed that, regardless of whether the foliation dips to the northeast or southwest, the stretching lineation remains stable, striking subhorizontally (SI-19–20), which eliminates the possibility of a thrust fault and indicates

that these foliations resulted from left-lateral movement. As shown in Fig. 3 and SI-21–27, the bending of the mylonite occurs along the northern slope of the mylonite belt, which can be projected downward to the foothills, where the RFD is located. It is notable that the deformation pattern of the mylonite as shown above and the overlying gypsum layers within the Wubang Breccia are highly similar, exhibiting top-to-north shear (Fig. 3). Therefore, this inferred normal fault, underlain by the mylonite bending to the north, can be determined as the southern prolongation of the RFD. Although the northern slope of the mylonite belt has been severely eroded, some low-angle normal faults can still be observed within the mylonite belt. For example, in the area 3000 m west of Honghe, the mylonitic rocks are seen to be cut by a low-angle normal fault dipping to the north, marked by a wide zone of fault gouge, along which the mylonite is decoupled and folded. This is interpreted to be the southward prolongation of the RFD (SI-28 and SI-29).

As shown in Fig. 5, our explanation of the origin of the outward bending of the mylonite suggests that the foliation dipping inwardly to the south is solely the overturned part of these folded foliations instead of resulting from outward thrusting, and originally they may also have dipped to the northeast at high angle like those along the northwest segment of the shear zone. In this manner, the disappearance of the escarpments along the middle segment of the metamorphic belt could have been caused by such tractional bending of the mylonite rocks (Fig. 6). These kinematic indicators suggest that the bending of the mylonite manifests itself as structural traction, dragged by the downward movement of the hanging wall (top-to-north shearing) along the overlying RFD, defined by the Wubang Breccia (Fig. 6). If valid, the bending of the mylonite can be classified as creeping

deformation.

The determination of the lineation feature of the mylonite belt has a double significance, demonstrating that oblique left-lateral shearing, despite a very small plunging angle, explains why the scale of the uplift and denudation of the Ailao Shan metamorphic belt increases from the northwest to the southeast, as indicated by more and more exposure of the syntectonic granite within the metamorphic rocks from the northwest to the southeast (Fig. 6). In addition, it testifies that the mylonite belt was drawn out from the deep crust underneath the Midu gap to the northwest, as proposed by Leloup et al. (1995), but that both uplift rate and denudation rate were low.
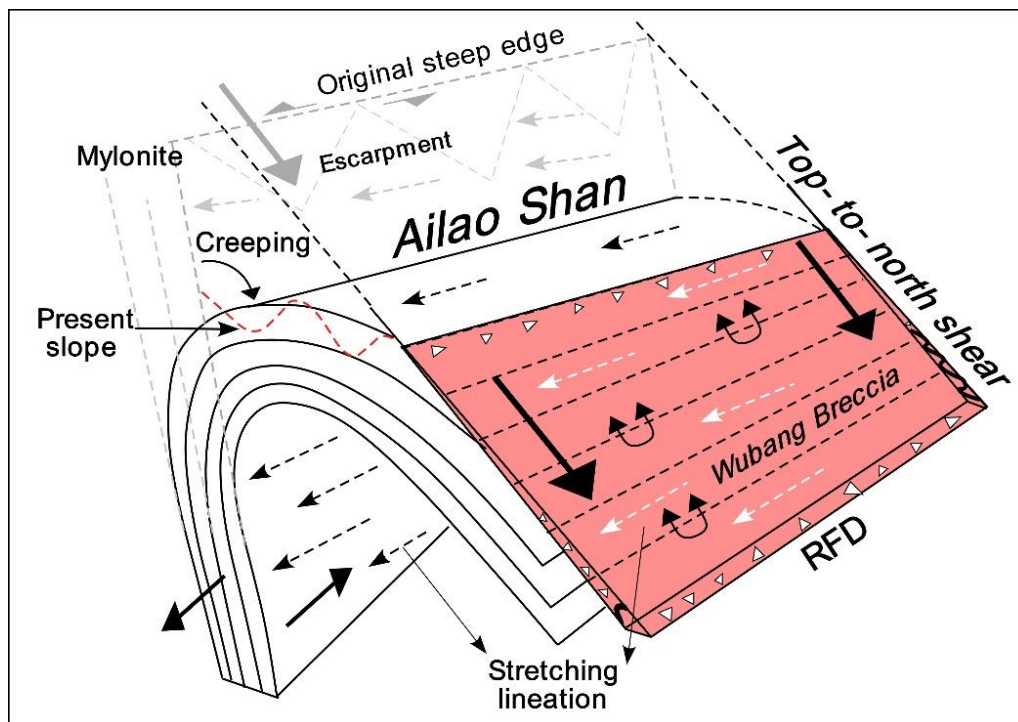
Figure 6. Geometric sketch of the bending mechanism of the mylonite in the form of creeping, dragged by the top-to-north shear along the RFD fault, developed along the Wubang Breccia. The black material represents the gypsum layers.

DEPOSITION OF THE LENGDUN CONGLOMERATE RESULTING FROM TOP-TO-NORTH SHEAR

Much of the Red River basin is floored by the Lengdun Conglomerate, which is drained through by the Red River and its numerous tributaries flowing to the southeast, being dismembered into a series of isolated linear hills (Figs. 3 and SI-8 and 30). Lithologically, it can be divided into three parts: From bottom to top, these are the Limestone Formation, Transitional Sandstone, and Ailao Shan Conglomerate (Schoenbohm et al., 2005). In our field study, the Honghe, Nasha, Lengdun, Niuduole, Wubangm, and Mosha areas were mapped in detail (Figs. 2 and 3) to determine the possible correlation between the sedimentation and deformation. Based on our field mapping and observations, the Langdun Conglomerate is mainly characterized as a monoclinic sequence, consistently dipping to the south, with dipping angle changing progressively from up to 70° SW to 5° from the base to the top of the sequence, as represented by the cross sections in the Honghe, Jiuhalong, Nansha, Lengdun, Wubang, and Mosha areas (Figs. 2 and 3).

The Lengdun Conglomerate is best exposed within the areas between Honghe and Nansha, overlapping the Late Paleozoic and Triassic rocks of the Yangtze block to the north (SI-35, 37 and 39) and resting on the Wubang Mudstone to the south along the RFD (SI-5–9) (Fig. 2 and Fig. 3). It is composed of coarse-grained alluvial and fluvial deposits, dipping to the southwest, with dipping angle decreasing upward (SI-33-34, 35-36, SI-37-38, 39-40). The Red River valley widens from Nasha to Dawenmi, being floored by the Lengdun Conglomerate, dipping to the southwest, with dipping angle decreasing upward (SI-35-36). In the Dawenti area (Fig. 3i-j), near the SE end of the Honghe basin, the

Lengdun Conglomerate is deformed into a syncline, also present with dipping angle decreasing upward (Figs. 3i and 3j). In the Nansha area, the Lengdun Conglomerate contains many large limestone blocks, characterized as landslide blocks (Figs. 3e and 3f). The Wubang Breccia pinches out from the Hongguang area to the northwest, where the Lengdun Conglomerate directly and consistently dips to the northwest against the mylonite and overlaps to the northeast the Triassic clastic rocks of the Chuxiong basin, decreasing in dipping angle upward (SI-33-34). However, such a change in dipping angle is not quite obvious in areas through which the Red River fault cut, probably because of its right-lateral movement (Figs. 2 and 3).

As shown above, one of the most prominent sedimentary features of the Lengdun Conglomerate is evidenced by the change in dipping angle, characteristic of syntectonic deposits, filling a growing asymmetric basin with consistently thicker strata on the southwest side closer to the ARSZ. Therefore, the revealed sedimentary features and geometry agree well our previous interpretation that the subsidence of the Honghe basin was controlled by the RFD with top-to-north shearing.

The Red River is considered to have a long evolutionary history, coeval with that of the ARSZ, and thus there must be an axial river running through the Red River basin (Clark et al., 2004). Indeed, in many places, we found many flat pebbles within the Lengdun Conglomerate in the central part of the valley consistently dipping to the west, evidencing paleoflow coming from the west along the center of the basin (Figs. 2 and SI-32). Based on this fact, we divide the Lengdun Conglomerate into three parts in the transversal direction: distal, axial, and proximal facies, respectively. The distal facies deposits are well

exposed along the northern flank of the Red River valley, being bounded by the three

tectonic elements of the Yangtze platform, with their contact relationship suggested as an

unconformity (Bureau of Geology and Mineral Resources of Yunnan Province, 1991) (Figs.

3 and 4 and SI-35, SI-37, and SI-39) and only locally cut by the faults (Schoenbohm et al.,

2006). This part of the succession is composed of poorly sorted breccias, with the detritus

varying from place to place, depending on the nature of the underlain bedrocks. The axial

facies deposits are a thick series of well-sorted pebble beds, which have the widest

distribution range within the Red River. Based on our field observation, the bulk of the

clasts within this part of the succession are made up mostly of sedimentary rocks, such as

limestone, quartzite, and sandstone, similar to those within the underlying Yangtze blocks

to the north. However, it locally contains well-sorted crystalline pebbles such as in the

areas of Honghe and Lengdun (SI-30-31). As shown in Fig. 3, whereas the Wubang Breccia

pinches out, the Lengdun Conglomerate directly contacts the Ailao Shan metamorphic belt,

but even so the conglomerate still does not contain metamorphic clasts shed from the Ailao

Shan metamorphic belt, but rather is dominated largely by fine-grained sedimentary clasts.

Ascertaining whether all clasts from the Ailao Shan exist in the lower part of the section

deposited proximal to the Ailao Shan would be useful, but these strata are mostly now at

depth and not exposed. However, in the area of Honghe within the central part of the

valley, there is a large outcrop of coarse-grained conglomerate exposed on the surface

along the trace of the Red River fault. It is composed of crystalline detritus and dips to the

south at a low angle (Figs. 2 and 3 and SI-30-31). We tentatively regard this outcrop as

an indicator of the proximal facies deposits that were originally buried under the axial facies

deposits and brought to the surface by the right-lateral transtensional movement along the Red River fault (Fig. 3).

Importantly, our field observations reveal that not only the dipping angle but also the grain size of the Lengdun Conglomerate decrease upward (SI-33–SI-40), with the top part composed of fine-grained lacustrine deposits, indicating that the high-energy deposition occurring within the Red River basin was gradually weakening.

DISPLACEMENT OF THE LANDSLIDE BLOCKS IN RESPONSE TO TOP-TO-NORTH SHEAR

The Honghe basin is bounded on the north by the Yangtze block along its southern tectonic elements, along which the Lengdun Conglomerate overlaps the bedrocks of Paleozoic and Mesozoic age. The main parts of these elements only experience minor deformation, as demonstrated by the flat-laying Paleogene red beds resting on the sedimentary cover rocks of Paleozoic and Triassic age (Fig. 1). In contrast, as shown in Fig. 1, the deformation is localized along their southern rims, where both Paleozoic and Mesozoic rocks were cut into many narrow strips in a complex mosaic by numerous NW-trending faults, along which they are repeated and stacked, being characterized as a thrust-fold belt and presenting as topography with high relief (Figs. 2 and 3 and SI-41, 44). They pass northward into the high mountains where they follow a series of narrow and steep-walled gorges, implying that these faults are young. In the area of Midu (Fig. 3), the northern boundary of the rim is clearly marked by a south-dipping thrust-fold belt, which places the Triassic clastic rocks northward on the Eocene red beds (SI-48), yielding a lower time constraint on the thrust-fold belt. Divided by the Yunajiang basin, the Chuxiong basin

and the Kunming block exhibit different geological features. Along the southern rim of the Kunming block, the strongly faulted rocks of Late Paleozoic and Triassic age are bounded on the north by a north-directed reverse fault, dividing the weakly deformed rocks with various ages to the footwall, and the rocks cut by it are highly brecciaed (Figs. 2 and 3 and SI-41, 43 and 44). Along the southern rim of the Chuxiong basin, the Triassic clastic rocks are folded into an anticline, holding up the Lengdun Conglomerate on its northwest flank, with the dipping angle decreasing upward (Fig. 3k and L, SI-33-34). The NE boundary of the anticline is marked by a southwest-dipping thrust fault, placing the Triassic rocks on the Jurassic rocks (SI-46), indicating that the deposition and shortening were correlated.

As shown above, the RFD plunges to the north under the Lengdun Conglomerate with the dipping angle decreasing upward, indicating that the RFD must have extended further to the north into the Yangtze block to create the space for the deposition of the Lengdun Conglomerate as syntectonic deposits (Fig. 3). Therefore, we tentatively assign the northern boundary fault of the thrust-fold belt developed along the southern rim of the Yangtze block as the toe of the RFD, which carried the bedrocks on the hanging wall onto the main part of the Yangtze platform. If this is the case, then all bedrocks on the hanging wall of the toe of the RFD can be defined as landslide blocks that dropped down from the high part of the Ailao Shan, coeval with the extension and subsidence of the Red River basin (Fig. 3). In addition, based on our field observations, the landslide blocks are not confined to the north of the Red River basin, but they also exist within the basin. As in Figs. 3c and 3d, in the Honghe area, a linear hill rises from the bottom of the Red River valley, enclosed by the Red River on the north and the Palong River on the south. The

central part of the hill is occupied by the Jurassic red beds, on which the Lengdun Conglomerate deposited, with the dipping angle decreasing upward and characterized as growth strata. The Jurassic red beds comprise sandstone and shale, which experienced intensive shearing, particularly the shale, in which all beddings have been replaced by cleavage. In the Nabing area (Figs. 2 and 3), the Jurassic rocks exposed along the northeastern end of the hill are overlain by Permian rocks along a north-dipping normal fault (SI-41-42). This indicates that these Jurassic rocks uplifted to the surface from under the Permian rocks and formed as a structural window, indicative of the superimposition of the different basement rocks of the basin. Note that these bedrocks, mostly limestone and basalt of Permian age, are bounded by the S-directed thrust fault on the north, which may marks the toe of the normal fault on the south, showing the northward displacement of the basement rocks (SI-41 and 43). As shown in Fig. 3, we interpret these sedimentary and deformation features to indicate that these bedrocks were formed as massive landslide blocks and pushed up to form a rolling anticline on the hanging wall of the RFD. If this is the case, then the age of the Lengdun Conglomerate yields a timing for the folding and uplift of the underlying massive landslide blocks. Moreover, as shown in Figs. 2, 3i, and 3j, from the area of Dawenmi to the southeast, a narrow strip of limestone of Triassic age crops out along the foothills of the Ailao Shan, separating both the Wubang Breccia and Lengdun Conglomerate from the mylonite belt. The limestone dips to the south at a high angle against the mylonitic belt, and those rocks in contact with the mylonite are sheared into a fault gouge. These Triassic limestones can be interpreted to be a large landslide block that dropped down from the top of the Ailao Shan metamorphic belt at the time of

folding, with the center of the syncline filled with Lengdun growth strata. As shown in Figs. 1 and 2, from the Lengdun Conglomerate to the southeast, the Honghe basin abruptly narrows and finally pinches out in the Lianghekou area. Accordingly, the landslide blocks on the north also pinch out at the end of the basin, indicating that the displacement along the end of the RFD decreased to zero.

Judging from this phenomenon and other geological constraints, the southern rim of the Yangtze block can be determined to comprise landslide blocks that rest on their weakly deformed counterparts along the toe of the RFD fault. As the massive landslide block sliding to the north along the RFD, the Red River basin began to develop its hanging wall, becoming filled by contemporary alluvial and fluvial deposits shedding from the Ailao Shan and aggraded from the north to south to have formed as growth strata. In this manner, the sedimentary age of the Lengdun Conglomerate yields a timing for the displacement of the landslide blocks.

ORIGIN OF THE RFD FAULT

The study of the mountain–basin coupling relationship between the Ailao Shan metamorphic belt and the Red River basin as shown above demonstrates that the range-front deformation and sedimentation along the NE range front of the Big Band of the ARSZ were not directly associated with the strike-slip movement. Rather, they were controlled by the N–S extension along the RFD fault with top-to-north shear. This shear bent the mylonitic rocks on the footwall to the north in the form of creeping deformation and controlled the deposition of the Lengdun Conglomerate on the hanging wall as growth strata. Based on this scenario, the deposition features of the Lengdun Conglomerate on

its hanging wall imply that the RFD fault underneath continues to extend northward into the Yangtze block and become exposed to the surface along the northern boundary of the southern rim of the Yangtze block. As such, the southern rim of the Yangtze block on its hanging wall can be defined as landslide blocks with their northward movement along the RFD creating space for the deposition of the Lengdun Conglomerate as growth strata. If this scenario is valid, the timing of both the top-to-north slip along the RFD fault and the occurrence of the massive landslide initiated during the Late Oligocene to Early Miocene. These processes were all controlled by gravitation, manifesting in the gravitational collapse of the Big Band. The resultant crustal materials, including alluvial and fluvial deposits and landslide blocks, accumulated in the range front of the Big Band. If so, then the Big Band of the ARSZ must be covered by the sedimentary cover rocks of the Yangtze platform in that time. The spatial correlation of the Red River basin with the Big Bang indicates that its formation was related to the change in geometry of the ARSZ, indicating that the ARSZ took its present geometric shape during the Middle Tertiary and, meanwhile, its left-lateral movement ceased.

As illustrated in Fig. 7, the northward movement of India with respect to South China creates a wide zone of right-lateral shear trending north–south, in which all crustal fragments are subject to clockwise rotation, including the ARSZ (Dewey et al., 1988; Lacassin et al., 1993; Huchon et al., 1994; Wang and Burchfiel, 1997). The Three River fold belt, bounded by the ARSZ on the northeast, is cut by many young or active left-lateral slip faults, trending NE–SW and NW–SE, respectively, including the Nandinghe, Heihe, Ruili, and Dien Bien Phu faults (Lacassin et al., 1998) (Fig. 7). These predict a bookshelf rotation

of crustal fragments around the vertical axis, including the Lanping–Simao basin, the

Lincang batholiths, and the Baoshan block (Wang and Burchfiel, 1997). The Lanping–Simao

basin was rotated as a nonrigid tectonic element, with large-magnitude rotations of up to

77° ± 11° reported by paleomagnetic, seismic, and structural studies (Lacassin et al., 1993;

Chen et al., 1995; Huang et al., 1992, 1993; Holt et al., 1991; Wang and Burchfiel, 1997;

Schoenhohm et al., 2005). As shown in Figs. 1 and 7, the Lanping–Simao basin,

characterized as a nonrigid tectonic element, experienced intensive shortening, particularly

its middle part, along which the Paleozoic rocks were pushed to the surface to form the

Wuliang Shan thrust-fold belt (WLF in Fig. 7). Its shortening is considered to have been

caused by the NE compression triggered by the rotation of the rigid Lingcang batholith

along the Heihe and Nandinghe strike-slip faults. As a result, the ARSZ bounding the

Lanping–Simao basin on the northeast was bent to the NW–SW direction. The effect of

such a rotation is profound, with its stress and strain fields penetrating northeastward

through the ARSZ to the southern part of the Chuxiong basin, whose rotation is exhibited

by the left-lateral shear along the Chuxiong fault (CXF in Fig. 7) (Schärer et al., 1990;

Burchfiel and Wang, 2003). If valid, the middle part of the ARSZ can be considered as an

extensional step-over in the left-lateral strike-slip domain. This resulted in an N–S extension,

leading to the gravitational collapse of its sedimentary cover rocks, accommodated by the

RFD. Originally, these rocks may have sat on the high part of the shear zone. As shown in

Figs. 3i and 3j, a strip of limestone of Triassic age is still preserved along the foothills of

the Ailao Shan, bounded by the mylonite on the south. This confirms that the mylonite

used to be covered by sedimentary rocks, but the displacement of the landslide blocks in

this region is limited.
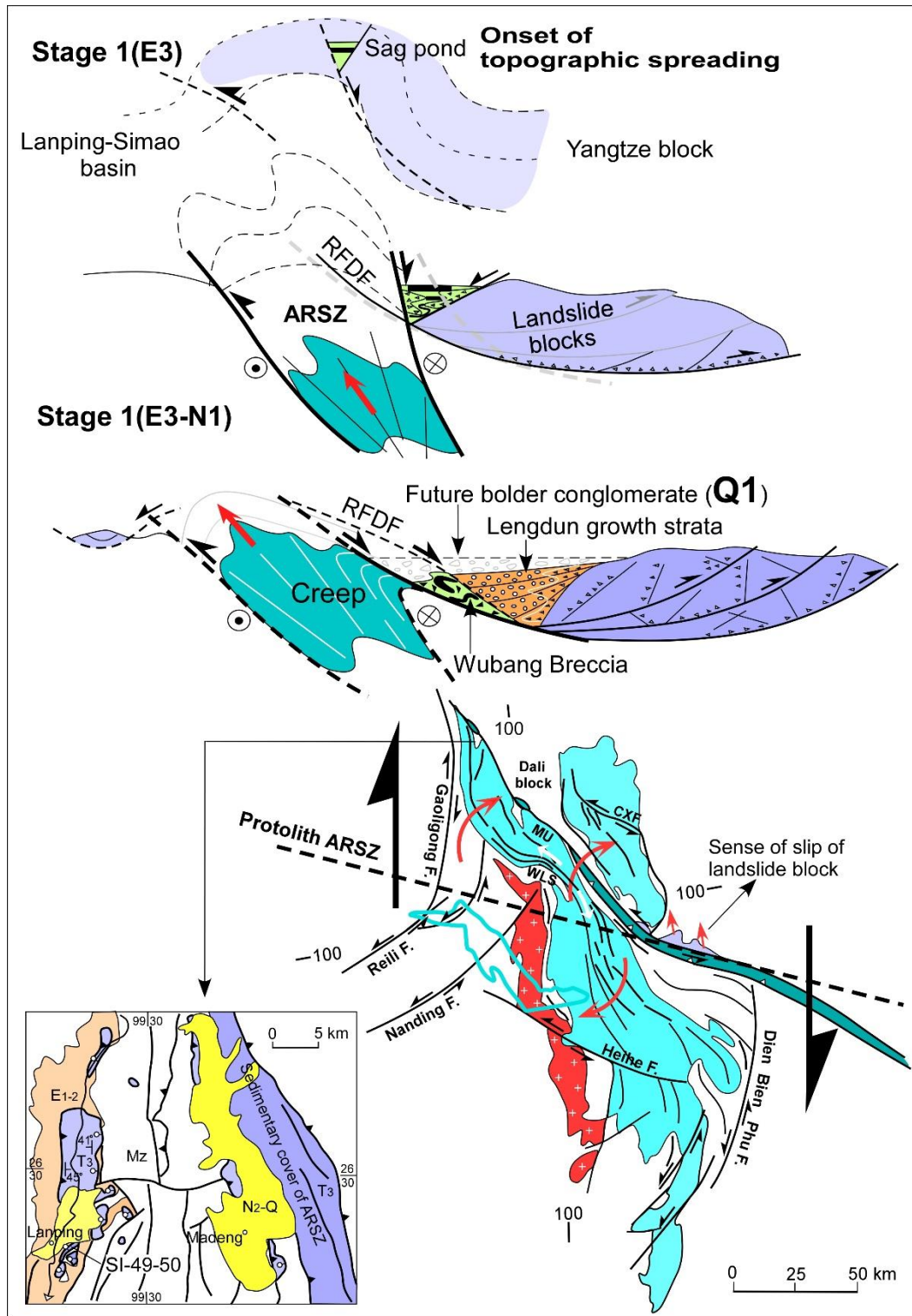
Figure 7. (Top) Model of the development of the RFD and associated deformation and sedimentation, controlled by the gravitational collapse of the Big Band of the ARSZ. (**Middle**) Tectonic map showing the differential crustal rotation and bending of the ARSZ and its adjacent tectonic elements resulting from the relative motion between India and

South China. It is speculated that the proto-ARSZ may strike straight in the NW–SE direction. The bending of the ARSZ triggered N–S extension along the Big Band, resulting in its gravitational collapse. CXF: Chuxiong fault; WLF: Wuliang Shan thrust-fold belt; MU: Midu gap. (**Bottom)** Simplified geological map of the central part of the Lanping basin, highlighting a series of klippens, with the largest area being 20 km^2. They are composed of limestone of Late Triassic age, underlain by younger rocks, with the youngest being Oligocene in age. These kinematic indicators (SI-50 and SI-51) show that they were transported from the east, where the ARSZ is located.

Based on the above study, the tectonic evolution of the ARSZ can be divided into two stages. The first stage occurred in the Early Oligocene. It was dominated by left-lateral motion with a minor vertical slip component, which led to the deposition of the Wubang Mudstone within the pull-apart basin or sag pond, confined within the uppermost crust. The revealed feature of the lineation within the Ailao Shan mylonite belt indicates that the left-lateral movement along the ARSZ only had a minor vertical slip component, present with a very low uplift rate. Consequently, the mylonite belt may be largely covered by sedimentary rocks at this stage, with the eroded debris carried away by the Red River. The second stage is characterized by bending, which led to the local extension generated along the Big Band. This resulted in the gravitational collapse of the sedimentary cover rocks sitting on the high part of the shear zone with steep topography, shedding of the landslide blocks into the piedmont, and deposition of the alluvial and fluvial sediments along the southern flank of the landslide blocks. As the down-slip motion of the landslide blocks continues, they gradually lost their gravitational potential energy, which can explain why the Lengdun Conglomerate exhibits an upward fining sedimentary feature. It is crucial to mention that the landslide blocks distributed within the Red River basin are not unique; they have counterparts scattered throughout the central part of the Lanping–Simao basin to the southwest of the ARSZ (Fig. 7) (Wang, 2006). They are composed of limestone of

Triassic age, with the youngest rocks on their footwall being Oligocene in age. They bear with the gypsum and are deformed into many rootless folds (Fig. 7 and SI-49 and SI-50). This is highly similar to the deformation of the Wubang Breccia, except that these rocks are overturned to the west, indicating that they were transported from the east, where the ARSZ is located (Fig. 7). We tentatively regard these klippens as landslide blocks that dropped from the top of the shear zone to the east, coeval with those dropping to the east.

CONCLUSIONS AND DISCUSSION

Identification of the sedimentary and deformational processes taking place along the NE range front of the Big Band of the ARSZ indicates that the stress and strain fields within this region were not dominated by strike-slip movement but by N–S extension, accommodated by the RFD with top-to-north shear, best defined by the Wubang Breccia. The effect of the top-to-north shear along it was profound, controlling the creeping of mylonite on the footwall and the coeval deposition of the Lengdun Conglomerate as growth strata on the hanging wall. The thrust fault belt bounding the Red River basin on the north is interpreted as comprising landslide blocks, with their northern boundaries marked by the toe of the RFD. Although their existence detained all streams shed from the Ailao Shan, their displacement created space for the Red River basin for the deposition of the Lengdun displacement. If this is the case, the deposition age of the Lengdun growth strata places a timing constraint on the displacement of the landslide blocks, and originally these landslide block sat atop the Big Band and dropped down as a result of topographic collapse. The extension was found to have resulted from the bending of the shear zone as a result of right-lateral shear between India and South China, occurring during the Late Oligocene

to Early Miocene. The upward fining feature of the Lengdun growth strata indicates that topographic collapse of the shear zone and associated top-to-north shear along the RFD fault ceased by the end of this time.

Although right-lateral movement along the Red River fault is demonstrated by numerous stream offsets (Allen et al., 1984; Replumaz et al., 2001; Schoenbohm et al., 2005), there is no trace of active tectonics along the Red River fault (Searle et al., 2010) and so the framework of the Lengdun growth strata is relatively well persevered. Particularly, there is no evidence indicating that the Red River fault underwent a significant vertical motion. Our finding is corroborated by the geomorphic study of Schoenbohm et al. (2004), which documents that the Ailao Shan uplifted only ~750 m in the Late Cenozoic. It is crucial to mention that a considerable amount of the crystalline detritus did not appear in the Red River basin until the Early Pleistocene, implying that the large-scale denudation of the Ailao Shan metamorphic belt occurred since that time, probably as a result of climate change. Note that the terrace deposits of Early Pleistocene age (SI-34 and 49) are preserved at an elevation of 1200 m, which is higher than any outcrop of the Lengdun Conglomerate, implying that much of the Red River basin used to be covered by the Early Pleistocene bolder conglomerate (Fig. 7).

References

Allen, C. R., Gillespie, A. R., Han, Y., Sieh, K. E., Zhang, B.,and Zhu, C., 1984, Red River and associated faults, Yunnan province, China, Quaternary geology, slip rates, and seismic hazard. Geological Society of American Bulletin, v. 95, p. 686-700.

Burchfiel, B. C. and Wang E., 2003, Northwest-trending, middle Cenozoic, left-lateral faults in southern Yunnan, China, and their tectonic significance, Journal of Structural Geology, v. 25, p. 781-792.

Burchfiel, B. C., Chen, L., Wang, E., and Swanson, E. (2008), Preliminary investigation into the complexities of the Ailao Shan and Day Nui Con Voi shear zones of SE Yunnan and Vietnam, Geological Society of American Special Paper, 444, p. 45-57.

Bureau of Geology and Mineral Resources of Yunnan Province, 1991, Regional Geology of Yunnan Province, Geological Publishing House, Beijing.

Chen, H., Dobson, J., Heller, F., and Hao, J., 1995, Palaeomagnetic evidence for clockwise rotation of the Simao region since the Cretaceous: A consequence of India-Asia collision: Earth Planet. Sci. Lett., v. 134, p. 203-217.

Dewey, 1., Shackleton, R. M., Chang, C., and Sun, Y., 1988, The tectonic evolution of the Tibetan plateau, in Chang, c., Shackleton, R. M., Dewey, 1., and Yin, 1., cds., The geological evolution of Tibet: Phil. Trans. Roy. Soc. London, Ser. A, v. 327, p. 379-413.

Harrison, T. M., Chen, W., Leloup, P. H., Ryerson, F.J., and Tapponnier, P., 1992, An early Miocene transition in deformation regime within the Red River fault zone, Yunnan, and its significance for Indo-Asia tectonics, Journal of Geophysical Research, v. 97, p. 7159-7182.

Harrison, T. M., Leloup, P. H., Ryerson, F. J., and Tapponnier, P., Lacassin, R., and Chen, W., 1996, Diachronous initiation of transtension along the Ailao Shan-Red River shear zone, Yunnan and Vietnam, In: T.M. Harrison and A. Yin (Editors), The Tectonics of

Asia, pp. 208-226, Cambridge Univ. Press, New York, NY.

Holt, W. E., Ni, J. F., Wallace, T. C., and Haines, A. J., 1991, The active tectonics of the eastern Himalayan syntaxis and surrounding regions: Jour. Geophys. Res., v. 96, p. 14,595-14,632.

Huang, K., Opdyke, N. D., Li, J., and Peng, X., 1992, Paleomagnatism of Cretaceous rocks from eastern Qiantang terrane: Jour. Geophys. Res., v. 97, p. 1789-1799.

Huang, K., and Opdyke, N. D., 1993, Paleomagnetic results from Cretaceous and Jurassic rocks of south and southwest Yunnan: Evidence for large clockwise rotations in the Indochina and Shan-Thai-Malay terranes: Earth Planet. Sci. Lett., v. 117, p. 507-524.

Huchon, P., Le Pichon, X., and Rangin, C. 1994, Indochina Peninsula and the collision of India and Eurasia, Geology, v. 22, p. 27-30.

Jolivet L., Beyssac, O., Goffe, B., Avigad, D., Lepvrier, C., Maluski, H., and Thang, T. T., 2001, Oligo-Miocene midcrustal subhorizontal shear zone in Indochina, TECTONICS, v. 20(1), p. 46-57.

Lacassin, R., Replumaz, A., and Leloup, P.H. 1998, Hairpin river loops and slip-sense inversion on Southeast Asia strike-slip faults, Geology, v. 26 (8), p. 703-706.

Leloup, P.H., and Kienast, J-R. 1993, High-temperature metamorphism in a major strike-slip shear zone: the Ailao Shan-Red River, People's Republic of China, Earth and Planetary Science Letters, v. 118, p. 213-234.

Leluop, P.H., Lacassin, R., Tapponnier, P., Scharer, U., Zhong, D., Liu, X., Zhang, L., Ji, S., and Trinh, P.T., 1995, The Ailao Shan-Red River shear zone (Yunnan, China), Tertiary transfer boundary of Indochina, Tectonophysics, v. 251: p. 3-84.

Leloup, P.H., Arnaud, N., Lacassin, R., Kienast, J.R., Harrison, T.M., Phan Trong, T.T., Replumaz, A., and Tapponnier, P., 2001, New constraints on the structure, thermochronology, and timing of the Ailao Shan-Red River shear zone, SE Asia, Journal of Geophysical Research, v. 106 (B4), p. 6683-6732.

Replumaz, A., Lacassin, R., Tapponnier, P., andLeloup, P. H., 2001, Large river offsets and Plio-Quaternary dextral strike-slip rate on the Red River fault (Yunnan, China), Journal of Geophysical Research, v. 106, p. 819-836.

Schärer, U., Tapponnier, P., Lacassin, R., Leloup, P.H., Zhong, D-L., and Ji, S., 1990, Intraplate tectonics in Asia: a precise age for large-scale Miocene movement along the Ailao Shan-Red River shear zone, China. Earth Planet. Sci. Lett., v. 97: p. 65-77.

Schärer, U., Zhang, L., and Tapponnier, P., 1994, Duration of strike-slip movements in large shear zones: the Red River belt, China, Earth Planet. Lett. V. 126: p. 379-397.

Schoenbolhm, L. M., Whipple, K. X., Burchfiel, B. C., and Chen, L., 2004, Geomorphic constraints on surface uplift, exhumation, and plateau growth in the Red River region, Yunnan Province, China, Geological Society of American Bulletin, v. 116, p. 895-909; doi: 10.1130/B25364.1.

Schoenbolhm, L. M., Burchfiel, B. C., Chen, L. and Yin J. 2005, Exhumation of the Ailao Shan shear zone recorded by Cenozoic sedimentary rocks, Yunnan Province, China, Tectonics, v.24, TC6015, doi:10.1029/2005TC001803

Schoenbolhm, L. M., 2006, Propagation of surface uplift, lower crustal flow, and Cenozoic tectonics of the southeast margin of the Tibetan plateau, Geology, v. 34, p. 813-816.

Searle, M., 2006, Role of the Red River Shear zone, Yunnan and Vietnam, in the continental extrusion of SE Asia, Journal of the Geological Society, London, v. 163, p. 1025-1036.

Searle, M., Yeh, M-W., Lin, T-H., Chung, S-L., 2010, Structural constraints on the timing of the left-lateral shear along the Red River shear zone in the Ailao Shan and Diancang Shan Ranges, Yunnan, SW China. v. 6(4): p. 316-338, doi: 10.1130/GES00580.1.

Tapponnier, P., Peltzer, G., and Armijo, R., 1986, On the mechanics of the collision between India and Asia, In Collision Tectonics, ed. M. P. Coward and A. C. Ries. Geological Society of London Special Publishing, v. 19, p. 115-157.

Tapponnier, P., Lacassin, R., Leloup, P. H., Scharer, U., Zhong, D., Wu, H., Liu, X., Ji, S., Zhang, L., and Zhong, J., 1990, The Ailao Shan-red River metamorphic belt: Tertiary left-lateral shear between Indochina and South China, Nature, v. 343, p. 431-437.

Wang, E., and B. C. Burchfiel,1997, Interpretation of Cenozoic tectonics in the right-lateral accommodation zone between the Ailao Shan shear zone and the eastern Himalayan Syntaxis, Int. Geol. Rev., v.39, p.191 – 219

Wang, E., Burchfiel, B. C., Royden, L. H., Chen, L., Chen, J., Li, W., and Chen, Z., 1998, Late Cenozoic Xianshuihe-Xiaojiang, Red River, and Dali fault systems of southwestern Sichuan and central Yunnan, China, Geological Society of American Special Paper, 327pp.

Wang, E., Wang, S., Fan, C., and Wang, G. 2006, Tectonic evolution of some Cenozoic klippen in west Yunnan, Chinese Journal of Geology, v.41(1), p.170-180.

Wang, Y., Zhang, B., Schoenbohm, L.M., Zhang, J., and Ai, S. 2016, Late Cenozoic

tectonic evolution of the Ailao Shan-Red River fault (SE Tibet): Implications for

kinematic change during plateau growth, Tectonics, doi: 10.1002/2016TC004229.

Supplemental informations-Photos

SI-5a: View west at the range-front detachment (RFD) fault, juxtaposing the Lengdun growth strata to the hanging wall and the Wubang Breccia to the footwall, 2000 m southwest of Dawenti.

SI-5b: View west at the Range-front detachment (RFD), dividing the Lengdun Conglomerate to the hanging wall and the fault itself is bent to the north as a result of its top-to-north shear and the none-rigid deformation the Wubang Breccia (E).

SI-6: View east at the Wubang Breccia, dividing the Lengdun Conglomerate to the hanging wall along its northern boundary fault, 500 m north of Nansha. Note that the fault is covered by undeformed alluvial deposits, presumably of Middle to Late Quaternary age, indicating the fault is no long active since then, 2000 m east of the Nansha.

SI-7: Photograph of the RFD fault, dividing the Lengdun Conglomerate to the hanging wall and the Wubang Breccia to the footwall, 2000 m south of Hongguang; see Fig. 2 for the location.

SI-8: View west at the Red River valley. The boundary of the Wubang Breccia with the Lengdun Conglomerate, dipping north at a low angle (25°), defined as the RFD fault. The isolated mountain in the background is composed of limestone of Triassic age, which bounds the Lengdun Conglomerate along the unconformity, dipping to the south at 75°, 1000 m east of Nansha.
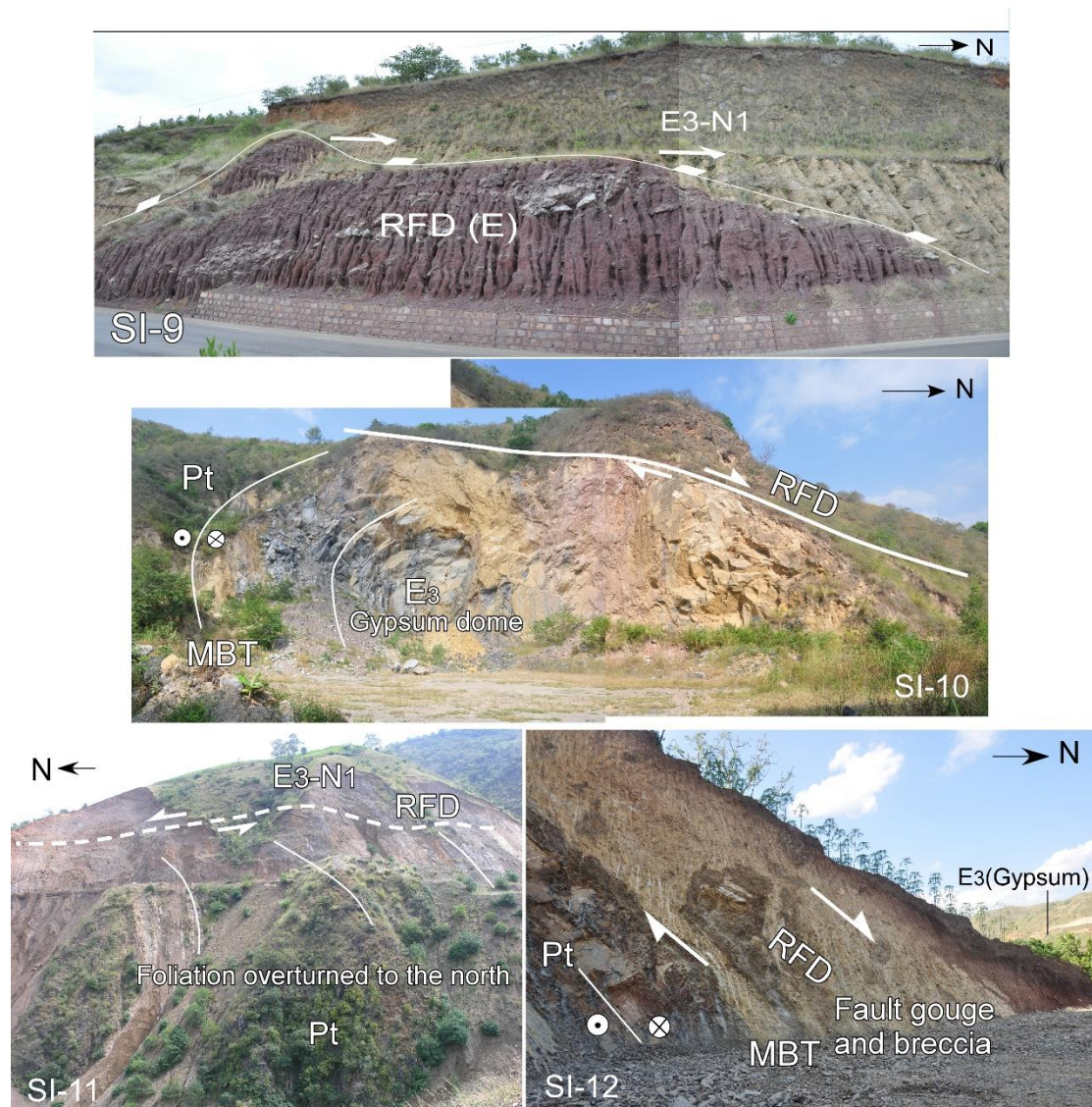

SI-9: View north at the RFD, dipping to the north at low angle, defined by the Wubang Breccia, dividing the Lengdun Conglomerate to the hanging wall, 2000 m west of Lengdun.
SI-10: View west at the boundary fault between the Wubang Breccia and mylonite (MBT), which is bent to the north, placing the mylonite on the gypsum dome and the latter is bent to the north consistently, 2000 m south of Lengdun.
SI-11: View southeast at the northern slope of the Ailao Shan, along which the Lengdun Conglomerate overlaps the mylonite along the RFD, formed as a

growth fault, and the mylonite underneath is bent to the north, in the area 1000 m south of Nabing.

SI-12: View west at the boundary fault between the Wubang Breccia and mylonite (MBT), which is cut by a wide zone of fault gouge and breccia, designated as RFD, in the town of Nansha.
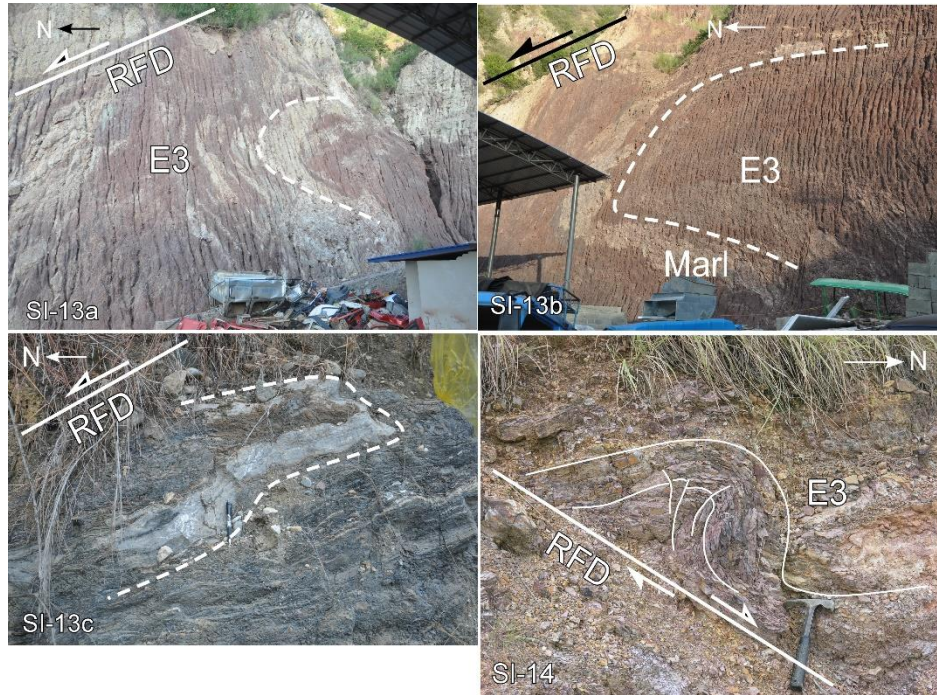
SI-13a–13b-c: Outcrop views of the Wubang Breccia, showing a series of gypsum and marl layers folded along a fold axis overturned to the north along their upper boundary fault, assigned to the RFD fault, 3000 m east of Nansha.

SI-14: Close-up view of the Wubang Breccia, which is folded and decoupled by a N-dipping low-angle normal fault, assigned to the RFD fault, 3000 m west of Honghe.
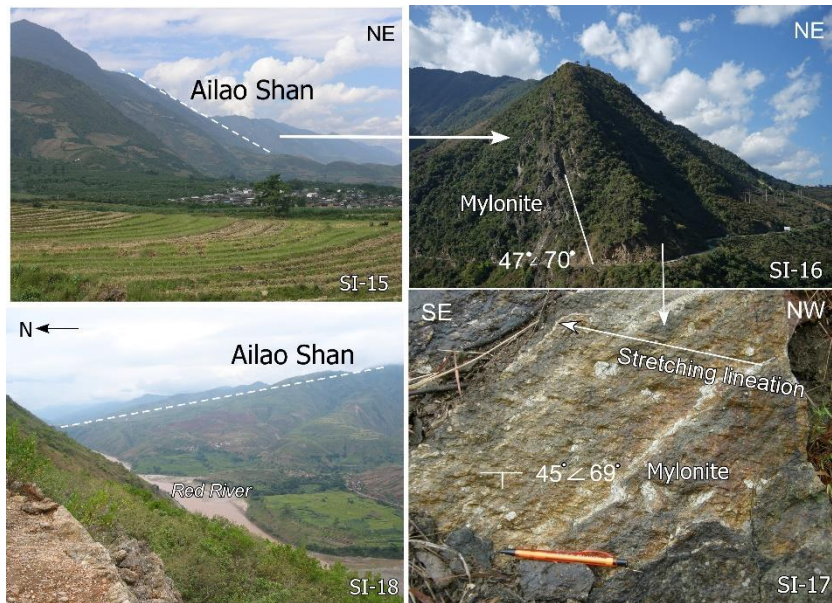
SI-15: Side view of the NE edge of the NW segment of the Ailao Shan metamorphic belt, featured by a series of triangular facets.

SI-16: View looking NW at the mylonite triangular facet bounding the NE edge of the Ailao Shan shear zone, located 5 km northwest of Gasa. Foliations of the mylonite on this facet dip to the NE at 65°.

SI-17: Close-up view of a foliation exposed along the triangular fault facet in SI-16 showing that foliations display stretching lineation plunging to the northwest at 20°.

SI-18: View southeast at the southern flank of the Big Band of the ARSZ, present with low topographic relief, in contrast with that of the NW segment of the ARSZ.

SI-19: View south of the S-dipping foliation exposed along the northern edge of the Ailao Shan, displaying subhorizontal stretching lineation, in the area 2000 m west of Nabing.

SI-20: View north of the SW-dipping foliation (originally interpreted as a thrust fault) of the Ailao Shan mylonite cropping out along its northeast edge, which bears the subhorizontal stretching lineation plunging to the NW at a 20° angle, in the Nabing area.

SI-21 and SI-22: View northwest at the NE edge of the Ailao Shan metamorphic belt, showing the outward bending of the mylonite bearing the subhorizontal stretching lineation and the top-to-the north shear sense along the northern slope of the Ailao Shan (RFD fault), in the area 200 m northwest of Nabing.

SI-23 and SI-24: View west at the mylonite exposed along the northern edge of the Ailao Shan mylonite belt, with the foliation bending to the north,

displaying subhorizontal stretching lineation and showing top-to-north shear sense, 2500 m west of Nanbin.
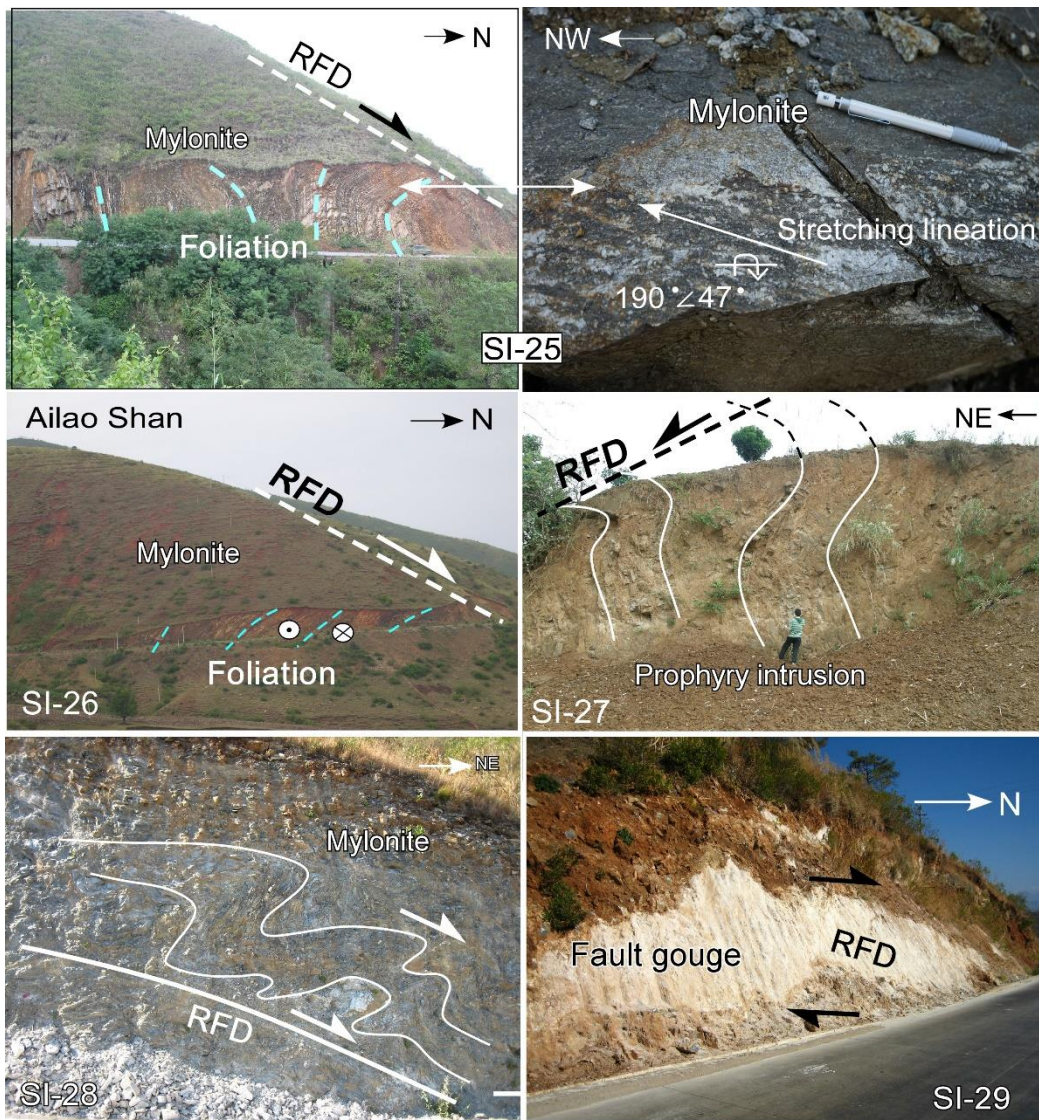
SI-25: View west at the mylonite cropping out along the NE edge of the Big Band, showing the foliation bending to the north, but the lineation remains subhorizontal, 3000 m southwest of Nanbin.

SI-26: View west at the northern edge of the Ailao Shan, showing the foliation of the mylonite being consistently bent to the north and the top-to-north shear, 4000 m west of Honghe.

SI-27: View east at a porphyry intrusion, intruded along the boundary between the Lengdun Conglomerate and mylonite belt, with the cleavages consistently bent to the north, showing the top-to-north shear.

SI-28: View west of the RFD fault that extends into the northern margin of the mylonitic belt, along which the mylonite are decoupled and folded,

overturned to the north, showing top-to-north shear; 5000 m southwest of Honghe.

SI-29: View north of the fault gouge and breccia, which marks the northern continuation of the detachment fault in SI-28, confined within the mylonite.
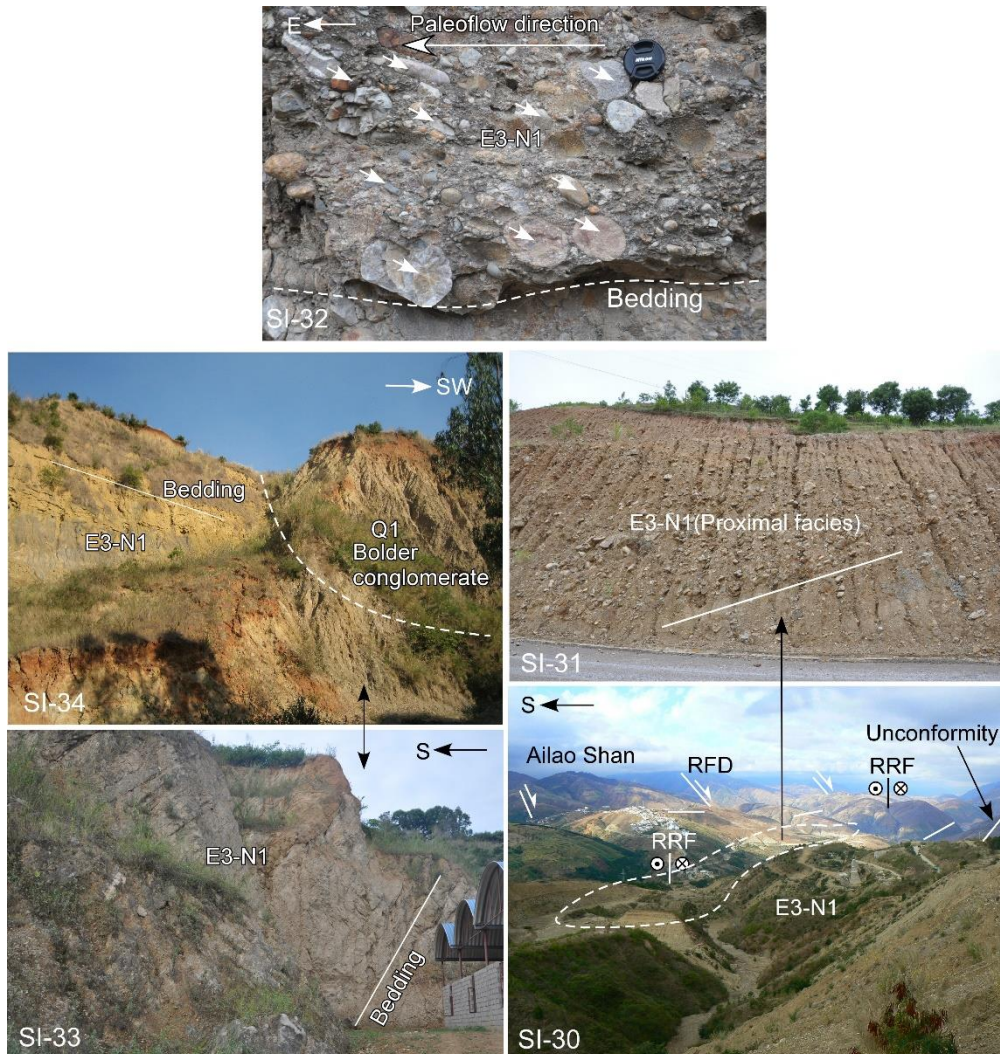
SI-30: View west at the Red River valley, floored by the Lengdun Conglomerate, which dips to the west with dipping angle decreasing upward.

SI-31: Coarse-grain conglomerate bearing crystalline detritus, probably proximal facies, exposed to the surface along the Red River fault.

SI-32: View south at the Lengdun Conglomerate cropping out in the central part of the succession, present with numerous flat pebbles consistently dipping to the west, from where the paleoflow came, located in an area 5 km west of the town of Honghe.

SI-33: View northwest at the basal part of the Lengdun Conglomerate, dipping to the southwest at a high angle, 3000 m south of Hongguang, see Fig, 2 for location.

SI-34: View south at the upper part of the Lengun Conglomerate, characterized by fine-grain lacustrine deposits, dipping to the south at a low angle against the mylonite, showing the feature of growth strata with SI-33. They are covered by the bolder conglomerate of Early Quaternary age in the Manfei area; see Fig. 2 for the location.
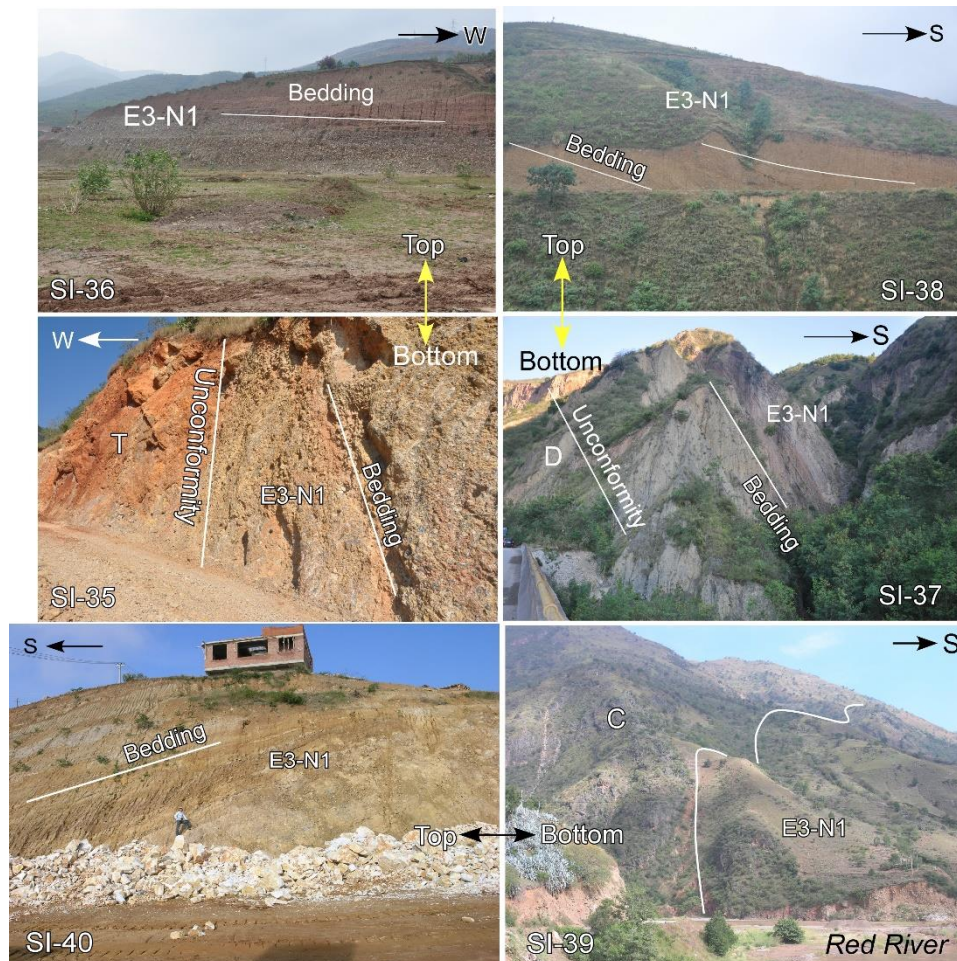
SI-35 and SI36: View north at the Lengdun Conglomerate, with its basal part consisting of limestone breccia dipping to the south at ~70°, and, moving to the south, the top part, the fine-grade fluvial deposits (view to the south) dip to the south at 10°, characteristic of upward fining growth strata, 5000 m north of Lengdun.

SI-37 and SI-38: View east at the coarse-grain basal part of the Langdun Conglomerate overlying limestone of Devonian age at 70°; the fine-grain upper part dips to the south 20° against the mylonite, defining an upward fining syntectonic sequence, 10 km east of Honghe.

SI-39 and SI-40: View east at the northern flank of the Red River valley, along with the Langdun Conglomerate (E3-N1), dipping to the south at 70°, with the dipping angle decreasing upward to 15° (with the bedding shown by

the blue line), characteristic of upward fining growth strata, in the town of Honghe.
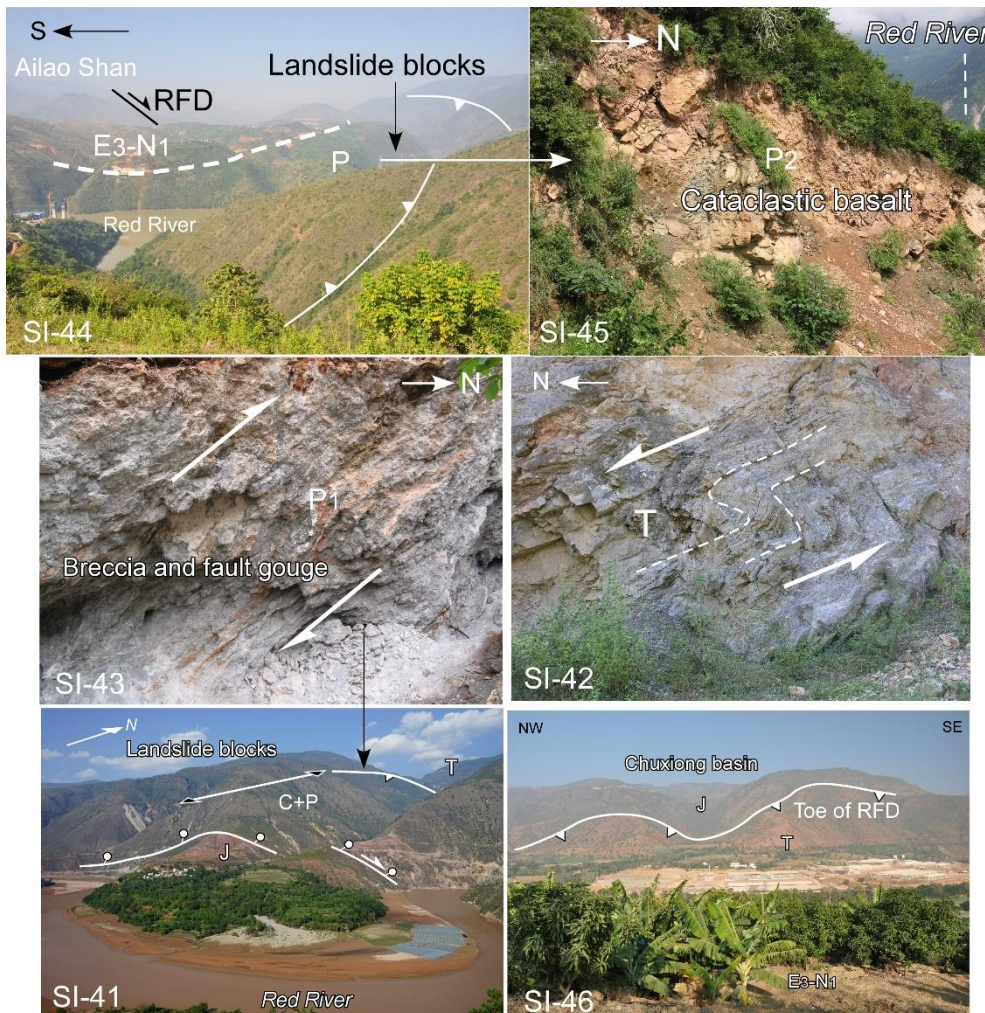
SI-41: View north at the northern flank of the Red River valley, present with high topographic relief, which is underlain by a series of crustal fragments of Late Paleozoic and Triassic age. The Permian rocks underlain by Jurassic red beds along a N-dipping normal fault, which are interpreted to be the landslide blocks, dropped down from the Ailao Shan mylonitic belt in the Nabing area.
SI-42: Outcrop view of the Permian limestone that experienced down-slip deformation along the normal fault on the hanging wall of the Jurassic rocks (SI-41) in the area north of Nabing.
SI-43: Close-up photograph of the breccia and fault gouge, which mark the northern boundary fault of a large landslide block, probably the toe of the normal fault in SI-41.

SI-44: View west at the Red River valley, showing an isolated hill in the center of the valley (Fig. 3E–F, underlain by Permian rock on the north and the Lengdun Conglomerate on the south; the former is considered to be a part of the massive landslide block，5 km north of Nansha.

SI-45: Close-up view of the Permian rocks in SI-44, which are brecciate, in contrast with the overlying Lengdun Conglomerate.

SI-46: View north at the northern boundary thrust fault (The tow of the RFD) of the anticline holding up the Lengdun Conglomerate in the Masha area, dividing the Triassic rocks to the hanging wall and the Jurassic rocks to the footwall.
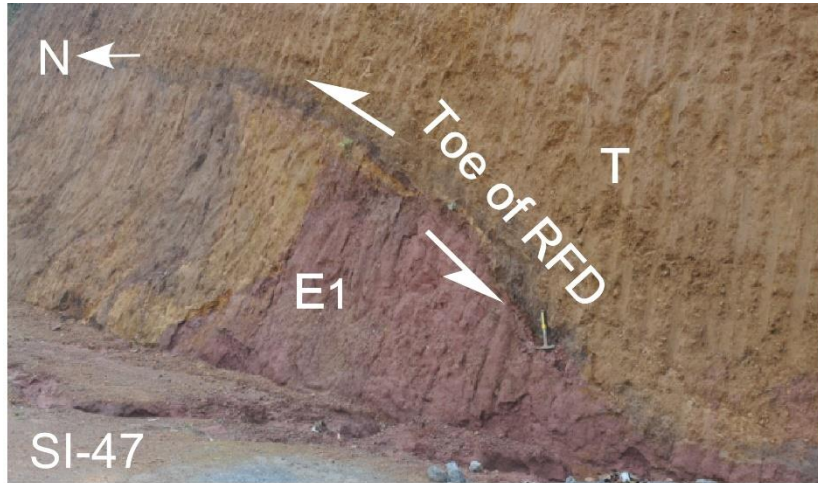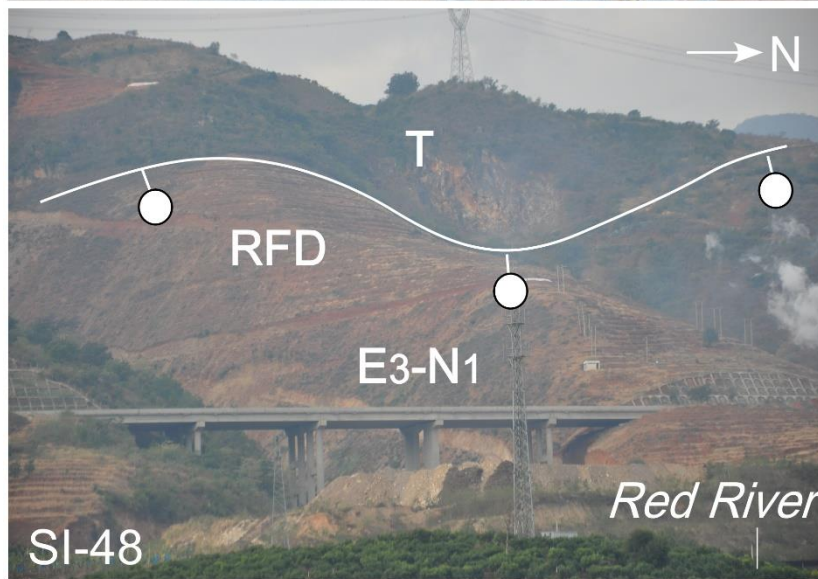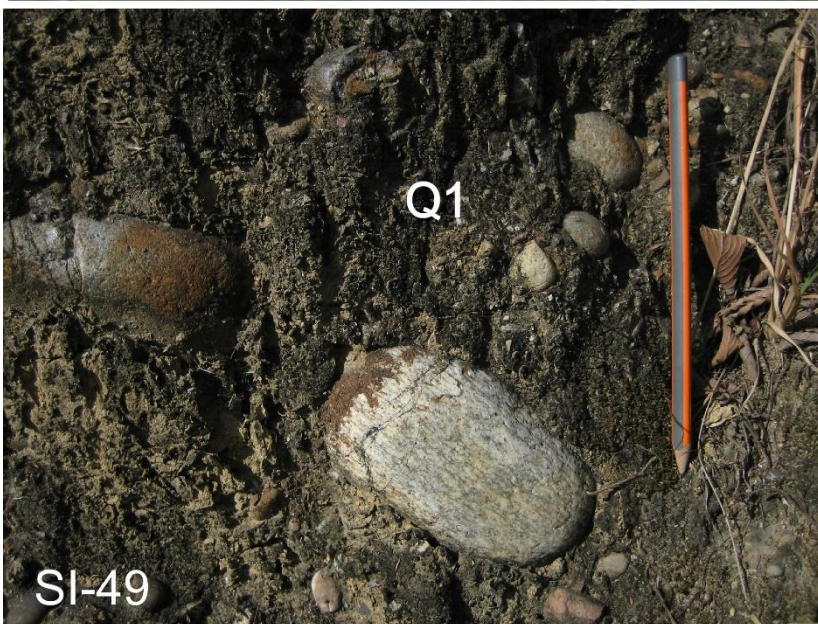
SI-47: Close-up view of the northern boundary fault (The tow of the RFD) of the southern rim of the Yangtze block, placing the Triassic clastic rocks （Landslide block） northward on the Eocene red beds.

SI-48: View south at the southern flank of the Ailao Shan, where the Lengdun Conglomerate is separated from the mylonitic belt by a strip of limestone of Triassic age, probably a landslide block.

SI-49: Close-up view of the bolder conglomerate of early Pleistocene age, standing as the highest terrace within the Red River valley.
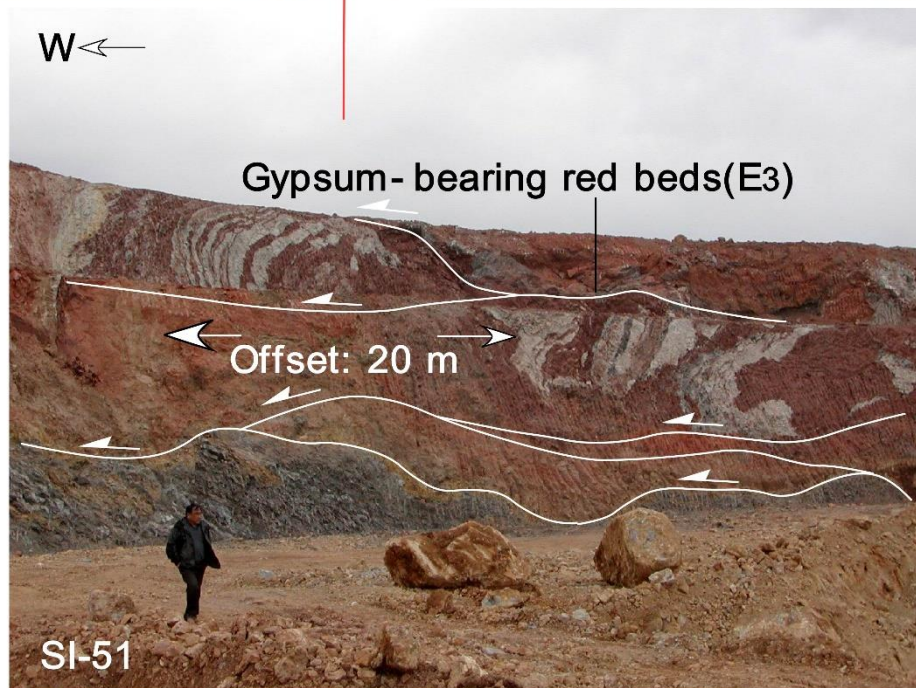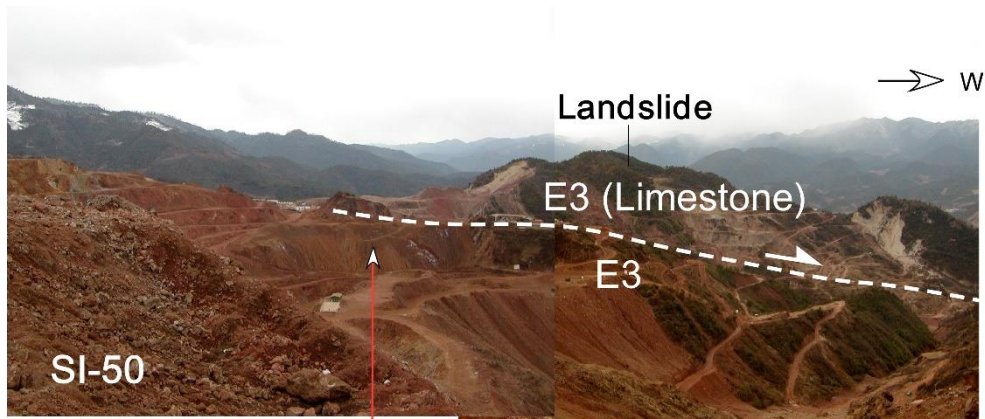
SI-50: Distal view of a landslide block broken into a series of pieces, comprising limestone of Triassic age; their down-slip movement to the west was accommodated by the underlain Eocene red beds and the contained gypsum layers were deformed into many recumbent folds overturned to the west, acting as a lubricant, 3 km southeast of the town of Lanping.

SI-51: View to the west at the outcrop of the Oligocene red beds within the Lanping area of the Landping–Simao basin (see Fig. 7 for the location). These rocks are strongly sheared into fault gouge and breccia and the contained gypsum layers are deformed into a series of rootless folds overturned to the

west, showing the direction of movement of the overlying landslide blocks; the location is the same as that in SI-49.

Supplemental informations-Tables

SI-Table A1. LOCATION OF OBSERVATION SITES AND ATTITUDE OF STRETCHING LINEATION

Site No.	Location		Foliation	Lineation
	Lat (°N)	Long (°E)	（Dip Azimuth°∠Dip°）	（Trend°∠ Plunge°）
STRETCHING LINEATION MEASURED FROM THE NE EDGE OF THE AILAO SHAN				
Majie-Mosha section				
P1	23°39.524'	101°50.920'	70∠69	147∠4
				338°∠2°
P3	23°46.511'	101°44.246'	65∠50	**340°∠9°**
				310°∠19°
P4	24°06.113'	101°30.412'	90∠51	160∠23
				130°∠15°
P5	24°15.503'	101°23.832'	65∠86	155∠6
P6	24°16.660'	101°22.614'	81∠62	158∠14
P7	24°20.688'	101°19.780'	65∠80	150∠16
P8	24°21.856'	101°18.715'	240∠65	**310∠9**
P9	24°22.269'	101°18.344'	51∠74	**341∠27**
				340∠14
P10	24°24.959'	101°16.149'	74∠65	150∠9
P11	24°26.052'	101°15.617'	40∠59	**317∠9**
P12	24°27.997'	101°13.792'	51∠56	125∠16
P13	24°30885'	101°11.595'	60∠47	**334∠6**
P14	24°33.237'	101°09.425'	73∠73	**349∠12**
P15	24°33.661'	101°08.916'	220∠73	**310∠5**
				344∠14
P16	24°34.223'	101°08.552'	60∠61	**324∠3**
P17	24°35.263'	101°07.827'	50∠48	**325∠5**
P18	24°36.146'	101°06.534'	53∠60	**331∠9**
			60∠79	**340∠11**
P19	24°36.877'	101°06.283'	53∠55	**328∠5**
P20	23°58.248'	101°36.779'	61∠71	**330∠9**
P49	24°52.768'	100°50.858'	244∠62	**275∠41**
			230∠51	**321∠41**
P50	24°59.091'	100°43.794'	56∠37	107∠14
Mosha-Honghe section				
P21	23°35.113'	101°57.605'	62∠59	**340∠8**
			62∠62	**321∠9**
				326∠7
P22	23°31.116'	101°01.987'	44∠50	130∠8
				116∠10

P28	23°58.248′	102°14.680′	328∠15	**266∠7**
				270∠5
P29	23°19.616′	102°30.465′	47∠57	97∠5
P30	23°22.388′	102°20.639′	59∠69	125∠20
P31	23°22.775′	102°20.026′	47∠72	120∠24
			45∠60	160∠27

Honghe-Manhao section

P32	23°19.513′	102°31.166′	220∠35	**297∠14**
				297°∠7°
P33	23°17.724′	102°37.395′	185∠69	115∠9
P34	23°17.113′	102°39.910′	187∠46	**270∠11**
			5∠62	**303∠21**
P35	23°15.911′	102°44.640′	210∠80	**310∠9**
P37	23°13.515′	102°49.200′	13∠70	**301∠11**
P38	23°13.766′	102°49.091′	35∠69	**325∠20**
			45∠80	**333∠24**
P39	23°12.633′	102°51.491′	231∠44	**345∠21**
			300∠11	**350∠45**
P40	23°12.169′	102°53.446′	24∠80	**290∠6**
P41	23°11.796′	102°54.041′	206∠48	**300∠5**
			215∠68	**309∠16**
P42	23°10.188′	102°57.291′	219∠56	**305∠13**
			213∠65	**300∠13**
P43	23°09.739′	102°57.770′	39∠61	130∠16
				341°∠7°
P44	23°07.698′	103°00.972′	227∠55	**315∠4**
			52∠66	**278°∠3°**
P46	23°01.066′	103°19.246′	45∠65	140∠25

STRETCHING LINEATION MEASURED FROM ROAD-SECTIONS ACROSS THE AILAO SHAN

Gasa-Zhenyuan section

1709-01	24°05.922′	101°30.913′	69∠52	125∠26
				115∠39
1709-02	24°05.566′	101°31.264′	39°∠52	128∠10
				126∠18
1709-03	24°05.038′	101°31.510′	55∠51	**289∠12**
				300∠10
1709-04	24°04.850′	101°31.361′	73∠56	**338∠16**
				330∠6
			54∠65	**331∠6**
				340∠9
1709-05	24°04.352′	101°31.741′	57∠61	**316∠13**
				303∠12
1709-06	24°04.003′	101°32.071′	60∠52	**320∠3**

				315∠8
1709-07	24°03.481′	101°31.729′	75∠57	155∠26
				158∠24
1709-08	24°03.184′	101°31.692′	64∠46	297∠4
				286∠9
1709-09	24°02.562′	101°31.676′	65∠54	335∠16
				320∠10
1709-10	24°01.882′	101°32.182′	78∠64	318∠14
				298∠16
1709-11	24°00.189′	101°32.446′	58∠59	140∠1
				145∠4
1709-12	23°59.118′	101°32.627′	50∠65	320∠5
				321∠1
			53∠49	326∠7
				329∠7
1709-13	23°58.684′	101°32.506′	65∠78	324∠5
				330∠10
1709-14	23°58.554′	101°32.191′	54∠58	334∠11
				315∠3
1709-15	23°58.385′	101°31.574′	63∠72	349∠6
				349∠4
1709-16	23°57.976′	101°31.882′	54∠42	324∠4
				347∠6
1709-17	24°01.400′	101°32.617′	43∠64	330∠13
				339∠13
1709-18	23°53.527′	101°39.921′	65∠47	310∠4
				295∠6
			69∠59	322∠8
				300∠10

Gasa-Mojiang section

1709-19	23°46.772′	101°44.516′	60∠56	330∠5
				332∠4
1709-20	23°46.560′	101°44.404′	67∠56	321∠4
				310∠9
			67∠59	326∠4
				336∠7
1709-21	23°46.453′	101°44.084′	70∠50	351∠3
				340∠10
1709-22	23°46.043′	101°42.678′	64∠84	347∠14
				333∠14
1709-23	23°45.994′	101°41.802′	75∠87	300∠11
				315∠8
1709-24	23°46.077′	101°41.392′	80∠60	288∠9
				296∠10

1709-25	23°45.805′	101°40.826′	80∠61	**335∠9**
				320∠12
1709-26	23°45.573′	101°40.687′	63∠45	150∠3
				154∠6
1709-27	23°45.313′	101°40.562′	76∠74	**275∠6**
				288∠11
1709-29	23°43.586′	101°40.909′	70∠76	159∠3
				140∠12

Yuanjiang-Mojiang section

1709-30	23°34.863′	101°57.211′	20∠81	**294∠16**
				300∠11
1709-31	23°34.193′	101°56.130′	57∠51	**289∠7**
				310∠6
1709-32	23°34.075′	101°56.054′	32∠64	**313∠7**
				316∠9
1709-34	23°34.055′	101°55.369′	35∠75	**315∠6**
				297∠19
1709-35	23°34.042′	101°55.366′	30∠84	121∠21
				126∠12
1709-36	23°33.236′	101°54.987′	66∠88	**331∠13**
				336∠18
1709-37	23°32.851′	101°55.098′	62∠83	**349∠10**
				355∠17
			38∠60	**328∠8**
				329∠12
1709-38	23°32.611′	101°54.912′	34∠75	**320∠8**
				323∠10
1709-39	23°32.149′	101°54.907′	45∠73	131∠20
				133∠14
1709-40	23°31.988′	101°55.042′	44∠82	**326∠19**
				325∠15
1709-41	23°31.083′	101°54.717′	32∠80	122∠14
				135∠19
1709-42	23°31.640′	101°54.427′	32∠86	115∠1
				129∠4

Yuanyang-Lvchun section

1709-44	23°14.134′	102°47.389′	25∠64	**291∠5**
				297∠5
1709-45	23°13.785′	102°46.770′	43∠46	**312∠11**
				323∠6
1709-46	23°13.262′	102°46.034′	38∠16	**341∠4**
				343∠2
1709-47	23°11.633′	102°44.735′	18∠64	**280∠5**
				277∠7

1709-48	23°10.869′	102°43.763′	115∠19	**334∠15**
				320∠12
1709-49	23°10.574′	102°43.532′	145∠38	201∠19
				206∠12
1709-50	23°09.614′	102°42.951′	115∠35	**328∠9**
				333∠10
1709-51	23°08.140′	102°40.575′	104∠14	**304∠8**
				307∠15
1709-52	23°07.464′	102°38.959′	47∠38	129∠8
				130∠10
1709-53	23°07.220′	102°38.689′	160∠40	181∠39
				191∠41
1709-54	23°07.114′	102°38.229′	64∠59	**309∠10**
				305∠14
Manhao-Jinping section				
1709-55	23°00.721′	103°19.220′	29∠66	121∠23
				120∠14
1709-56	23°00.088′	103°19.182′	52∠54	**321∠7**
				339∠3
1709-57	22°59.736′	103°18.638′	226∠39	**289∠2**
				300∠5
			254∠54	**274∠34**
				289∠10
1709-58	22°59.253′	103°18.536′	359∠32	**308∠3**
				320∠1
1709-59	22°59.074′	103°17.894′	199∠49	**317∠4**
				314∠6
1709-60	22°58.301′	103°17.357′	27∠70	**316∠12**
				315∠9
1709-61	22°57.763′	103°17.821′	229∠50	**325∠15**
				310∠10
			226∠44	**325∠11**
				339∠15
1709-62	22°57.248′	103°17.180′	31∠58	85∠54
				100∠45
1709-63	22°56.684′	103°14.819′	207∠55	116∠2
				108∠4
1709-64	22°56.727′	103°13.728′	79∠63	126∠18
				140∠24

Note: All 196 stretching lineation measurements consist of 143 measurements that plunge to NW (bold) and 53 that plunge to SE.

Fisher Vector Distribution

The standard mean vector calculation is conducted by using STEREONET 9.6.1 (by Richard W. Allmendinger). The uncertainty intervals are calculated from the following equation:

$$\cos \delta\alpha_p = 1 - \left(\frac{N-R}{R}\right)\left[\left(\frac{1}{1-p}\right)^{\frac{1}{N-1}} - 1\right]$$

Where p is the probability, N is the number of observations, and R is the resultant vector length. Kappa, κ, the dispersion or concentration factor, is estimated from one of the following caculations:

$$\kappa \approx \left(\frac{N}{(N-R)}\right)\left(1 - \left(\frac{1}{N}\right)\right)^2 \quad for\ N < 16$$

$$\kappa \approx \left(\frac{N-1}{(N-R)}\right) \quad for\ N \geq 16$$

Stereonet 9.5 uses $(N-1)$ following Fisher's original estimation (Fisher *et al.*, 1987; Davis, 2002).

All 196 measurements contain 143 that plunge to NW and 53 that plunge to SE.
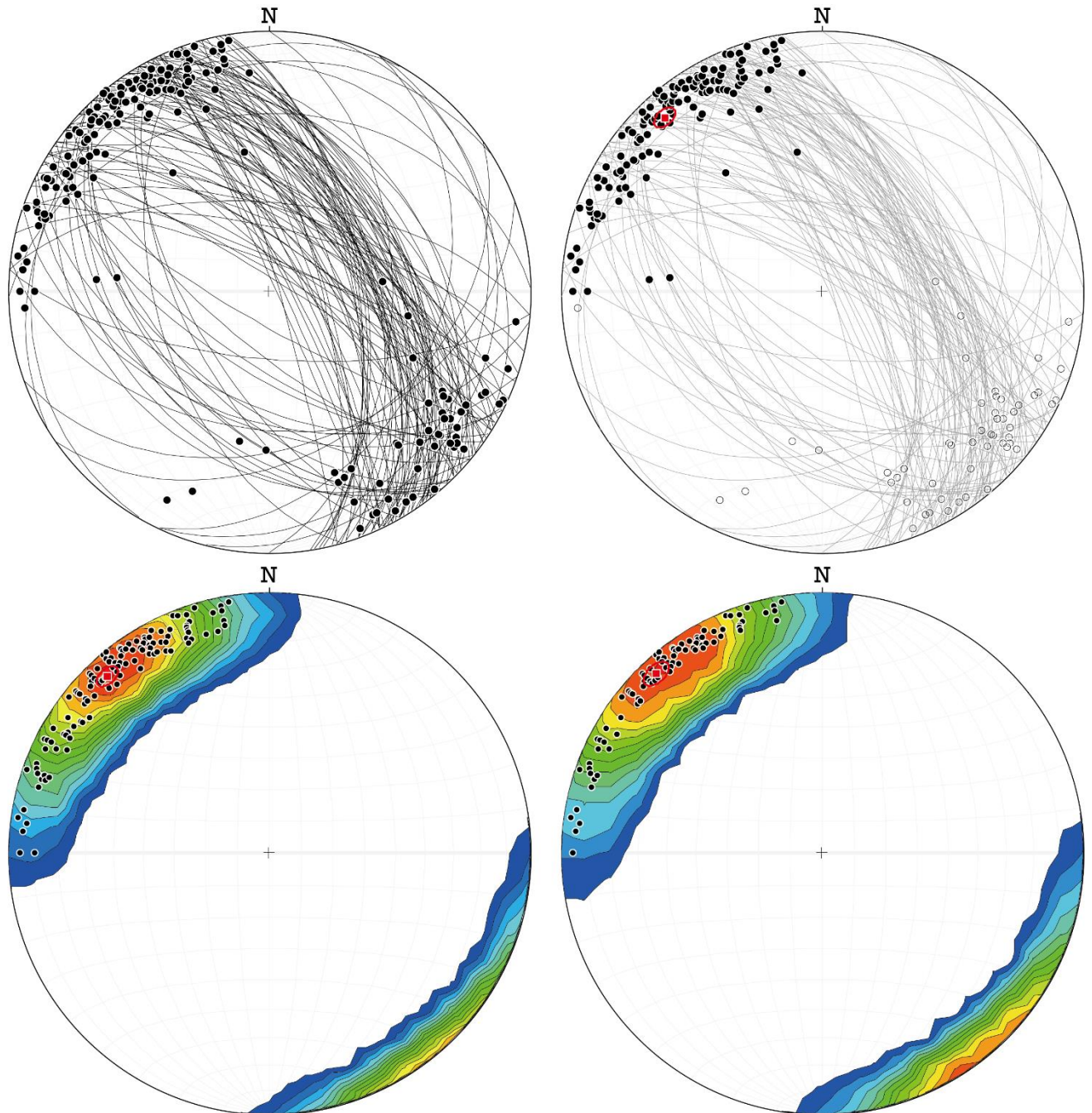
Figure A1. a: Stereonet plots (Low hemisphere) showing the orientations of all 115 foliation and 196 lineation measurements from the Ailao Shan metamorphic belt. b: Stereonet plots (Low hemisphere) illustrating the orientations of 143 NW-plunge lineations and 53 SE-plunge lineations (hollow). Red circle shows the Fisher Mean Vector of all NW-plunge lineations. c: Kamb contouring and Fisher Mean Vector of 125 NW-plunge lineation less than 15 °. d: Kamb contouring and Fisher Mean Vector of 90 NW-plunge lineation less than 10 °. See Table A2 for Fisher Mean Vector calculation results.

Table A2 FISHER MEAN VECTOR OF LINEATION MEASUREMENTS

Group	Number	Trent (°)	Plunge	α95	α99	κ	Mean length

All NW	143	317.9	10.8	3.0	3.8	16.2	0.9388
Other	53	136.6	18.0	7.2	9.0	8.3	0.8816
NW≤10°	90	317.3	6.8	3.5	4.4	18.8	0.9474
NW≤15°	125	317.6	8.7	3.0	3.7	18.6	0.9468

References

Davis, J.C., 2002, Statistics and data analysis in geology: Hoboken, NJ, John Wiley, 638 p.

Fisher, N.I., Lewis, T.L., and Embleton, B.J., 1987, Statistical analysis of spherical data: Cambridge, Cambridge University Press, 329 p.